ISSN : 0019-5693

INDIAN JOURNAL
OF
THEORETICAL PHYSICS

VOLUME 71 **NOS. 1, 2**

JANUARY, 2023 – JUNE, 2023

Published by the
CALCUTTA INSTITUTE OF THEORETICAL PHYSICS
(Formerly, INSTITUTE OF THEORETICAL PHYSICS)
"BIGNAN KUTIR"
4/1, MOHAN BAGAN LANE, KOLKATA-700004

(Peer-reviewed Journal)

ISSN : 0019-5693

INDIAN JOURNAL
OF
THEORETICAL PHYSICS

[Founder President : Late Prof. K. C. Kar, D. Sc.]

VOLUME 71 **NOS. 1, 2**

JANUARY, 2023 – JUNE, 2023

INDIAN JOURNAL
OF
THEORETICAL PHYSICS

"BIGNAN KUTIR"
4/1, MOHAN BAGAN LANE, KOLKATA-70004, INDIA

SUBSCRIPTION RATE

INDIA : For Library (Institute)

₹1500.00 for each volume

FOREIGN : $ 350 for each volume

Drafts, Orders, Enquiries & Claim for Non-Receipt of Journal should be sent to :

CALCUTTA INSTITUTE OF THEORETICAL PHYSICS
(Formerly, INSTITUTE OF THEORETICAL PHYSICS)
"BIGNAN KUTIR"
4/1, MOHAN BAGAN LANE, KOLKATA-700004, India

C O N T E N T S

INDIAN JOURNAL OF THEORETICAL PHYSICS, VOL 71, NOS. 1 & 2, 2023

QUANTUM MATERIALS

* Pritam Deb
Department of Physics
Tezpur University (Central University)
Tezpur 784028

Abstract : 2D vdW quantum systems are stable under ambient conditions, exhibit high crystal quality, and are continuous on a macroscopic scale suitable for many technological functionalities. In layered 2D vdW heterostructure systems, valley (K or K0) and sublattice (A or B) provide tunable binary degrees of freedom to modulate the electronic properties leading to topological surface effects, such as the significant quantum Hall effects. Moreover, the 2D honeycomb layers are prone to form various crystallographic reconstructions, with structural variations as compared to their pristine monolayer system. On the other hand, their distinct electronic properties around the Fermi level and their topological properties are affected due to substrate hybridization effect. Magnetism in these 2D materials as case of metal-free magnetism is now area of particular interest due to small spin-orbit coupling and long spin scattering length. The physics of magnetism in magnetic atom free 2D vdW materials and their respective heterostructures is yet to be revealed in a wide range of systems. The long spin flip length of 2D quantum systems has made them potential candidates for spintronic applications where the spin orbit coupling plays important role for electronic device applications. As 2D layers are held together by vdW force, the realization of respective heterostructures offers a rich platform to study fascinating vdW force-driven properties, like, electronic structure and band structure, magnetic and transport properties, spin-orbit coupling or exchange coupling and topological properties induced by proximity effect and catalytic behaviour. Thus, investigation on electronic structure, topological effects and magnetic behaviour of the 2D quantum systems (both monolayer and heterostructure) is one of the active and emerging current research field.

** Prof. K.C. Kar Memorial Lecture delivered by Prof. Pritam Deb, Dept. of Physics, Tejpur University in one day seminar on 'Recent Trends of Physics & Mathematics' held on 7 July, 2023.*

1. Two Dimensional van der Waals Quantum Systems

Dimensionality is one of the most defining material parameter. However, reducing the dimensionality of a system is often related with exceptional electronic, topological and magnetic properties because of the reduction of available phase space and reduced screening lead to enhanced quantum effect and increased correlations in the systems. As a result, chemical compounds can exhibit dramatically different properties depending on their arrangement in zero dimension (0D), one dimension (1D), two dimension (2D) or bulk three dimension (3D) structure. Although quasi-0D e.g. cage molecules, quasi-1D e.g. nanotubes and 3D objects are extensively studied, 2D materials are now gaining interest for interesting research among these class of materials. Besides, the condensed matter community extensively investigated the Physics of quasi-2D systems that host the fractional quantum Hall eect before the discovery of stable 2D materials. Atomically thin 2D materials, like graphene and its analogues, such as hexagonal boron nitride (h-BN); phosphorene and its analogues, such as the transition-metal dichalcogenides (TMDCs) are presently attracting the research focus because of their fascinating and unique electronic structure which is modulated by van der Waals (vdW) interaction force (shown in Fig. 1). In general, these 2D structures achieve stable geometry and exhibit high crystal quality under ambient conditions in confined dimension, termed as 2D vdW quantum systems, which are suitable to design respective 2D vdW heterostructures. The vdW heterostructure specializes in various potential properties, such as vdW interaction, strong Coulomb interaction, layer dependence, dielectric screening engineering, work function modulation and phase engineering. These properties help the

vdW heterostructures to be explored in various direction with many applications.

Considering the advances in high performance computing and mathematical algorithms, First-principles methods (to model dense and sparse matter) are paramount not only to the discovery and design of new 2D materials, but also for developing our understanding and control of growth morphology. Despite the reliability and accuracy of quantum chemical (QC) and quantum Monte Carlo (QMC) calculations, density functional theory (DFT) still remains the workhorse for exploring larger and more complex systems with significant atomic relaxations such as the graphene, dichalcogenides and related vdW heterostructure systems. Computationally, the scaling of many existing quantum mechanical methods with respect to the system size hinders their applications to large systems like 2D heterostructures in nanoscale range. Thus, quantum mechanical methods like, DFT and tight-binding (TB) basis are preferred to investigate the electronic structure, topological behaviour and magnetism in these 2D quantum systems with varying degrees of computational demands and transferability and with successive developments approaching chemical accuracy. In this aspect, DFT is fairly accurate First principle based method for electronic structure calculation using pseudopotential wave basis, while TB model is taking full potential wave basis. As a result, both DFT and TB form an ideal and generalized option to analyze various properties of these complicated and realistic 2D systems. However, these modern DFT-based approaches are now mature enough with proper caution. Thus, it is possible to use theory to explore the classes of layered vdW materials, where vdW interactions are intrinsically important, and thereby placing us on the

verge of a new era in computational aided materials research. Besides, these 2D materials can be realized experimentally via epitaxial grow process through deposition technique to correlate with the theoretical simulations for various properties (i.e. structural, electronic, magnetic, thermal, topological, transport, catalytic). In this aspect, theory based simulation and experimental analysis can be corroborated to practically understand these 2D monolayer and heterostructure systems in quantum regime.

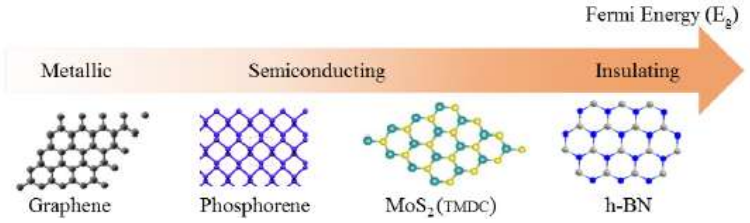

Figure 1
The library of two-dimensional materials, including graphene and its analogues; with an increasing bandgap (in terms of Fermi energy, E_g) from left to right shown in gradient color arrow.

2. Electronic Properties of 2D Quantum Systems

It is obvious that research on graphene has not only rapidly developed in the past decade into a vast research platform that encompasses solid state physics, materials science and engineering, but it has also sparked immense curiosity in a wide range of 2D layered materials with diverse electronic properties. Besides, graphene exhibits unique band structure and exceptionally high carrier mobilities that make it a unique platform for exploring Low Dimensional Physics and for creating a new generation of electronic devices with atomically thin geometry with many drawbacks that have yet to be overcome. In this

aspect, other 2D layer materials introduce more versatility, including conductors, semiconductors with varying bandgaps ranging from 0.5 eV to 3 eV (i.e. phosphorene, MoS_2) and insulators (i.e. h-BN). This broad world of 2D vdW materials with selected finite material properties opens up the possibility of heterostructure assembly at the atomic scale (i.e. quantum regime), creating novel heterostructures that display totally new Physics concepts and enable unique functionalities. In general, the fascinating behaviour of low dimensional systems is more prominent in atomically thin materials and indeed, graphenes unique electronic properties rise from its reduced dimensionality. The quantum mechanical description of the electronic band structure can be simplied by introducing quasi-relativistic particles near the corners of the Brillouin zone, as shown in Fig. 2(a). Therefore, graphene quasiparticles move like electrons that have lost their mass, except that the speed of light is replaced by graphene Fermi velocity, which is some three hundred times smaller. This nature gives rise to many interesting features for graphene electronics and its integration for vdW heterostructure. Besides, the two carbon atoms in the graphene unit cell are replaced by boron and nitrogen atom, respectively which breaks the inversion symmetry in h-BN (shown in Fig. 2(b)). As a result, a large energy gap opens at the valleys, making h-BN an extremely good dielectric and insulator with wide bandgap. Similarly, the electronic structure of MoS_2 consists of one layer of a transition metal molybdenum (Mo) sandwiched between two layers of sulfur with a thickness of 2-3 Å. It has no inversion symmetry, thus retains a finite nonzero bandgap. However, the electronic band structure is complicated due to the strong spin orbit coupling (SoC) interaction, which arises from the high orbital velocities of partially filled

d subshells in the relatively heavy Mo atom (shown in Fig. 2(c)). Considering the case of phosphorene, a layered allotrope of elemental phosphorus, has some interesting properties that arise from its inherent in-plane structural anisotropy (shown in Fig. 2(c)) due to the form of puckered geometry. Consequently, it has an anisotropic electronic band structure, and its charge carriers have anisotropic effective mass. The existing anisotropy has a strong coupling with the lattice strain leading to suitable application of the system as low-dimensional piezoelectricity.

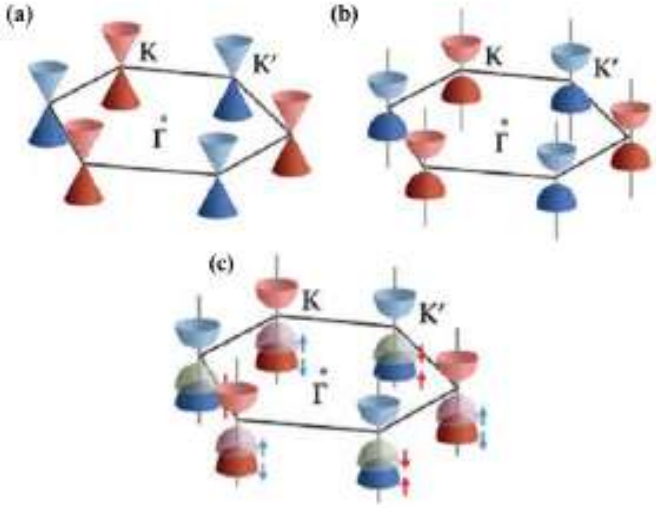

Figure 2

Schematic representation of electronic band structures at the corners of the first Brillouin zone for (a) graphene sheet (conductor), (b) h-BN (insulator with wide band gap) and (c) semiconductor (MoS_2 and phosphorene) with finite band gap.

3. Topological Behaviour of 2D Quantum Systems

In 2D vdW systems, topological ordering is analogous to a conventional 2D electron gas subject to a strong external magnetic field causing electronic excitation gap at the boundaries or surfaces. By definition, topological insulator (TI) is a material that has a nontrivial

symmetry-protected topological order resulting in metallic surface states having Dirac-like spectrum (shown in Fig. 3). In this phase, the electronic band structure is typical to that of an insulator with the Fermi level in between the valence and conduction band. Furthermore, Spin-orbit interaction plays significant role in tuning this behaviour. A specific topological invariant (Z2) is used to distinct between 2D and 3D topological insulators, which defines the ground state of the system. The spin must be either parallel or antiparallel to the particle momentum in real relativistic spin-1/2 fermions. In this line, quasiparticles (at K or K' valleys) in graphene have an analogous pseudo-spin degree of freedom, which describes the wave function symmetry on the two triangular sublattice of graphene hexagonal lattice. From that chiral nature of charge carriers in the system, various electronic properties emerge leading to topological phases and its transformation, such as a half-integer shift in the quantum Hall effect or Klein tunnelling. As a result, non-trivial topological Berry phase is detected first experimentally in graphene, which supplies an important connection to the later discovery of topological insulators. Similar, topological phases can be expected in h-BN system due to its wide electronic bandgap and inversion symmetry, like graphene sheet. The SoC interaction factor splits the valence bands of MoS_2 into two spin polarized bands (i.e. twice the number of spinor). Here, time-reversal symmetry (TRS) requires the spin and momentum degrees of freedom to be coupled with each other such that the K and K' valleys carry opposite spin polarizations. That unique spin and valley texture causes electrons to experience a pseudomagnetic field, which gives rise to distinct topological trivial phases (i.e. so-called valley Hall effect) without applying any external field. Furthermore, both electron

spin and momentum valley of the electrons in the system can be controlled by applying circularly polarized light to tune its property as per potential functionality in the field of spintronics application. Similar, topological behaviour can be logically explained in the anisotropic phosphorene system due to its _finite nonzero electronic bandgap in semiconducting range and TRS, like MoS_2 sheet. Moreover, quantum confinement and the lack of bulk dielectric screening have profound effect on the optical phonon properties of semiconducting phosphorene. Here, the phosphorene monolayer undergoes a transition to a direct electronic bandgap leading to relatively stronger optical phonon absorption and more efficient radiative recombination. This nature provides interesting feedback to consider the novel electron-phonon interaction and respective phonon population distribution in monolayer system.

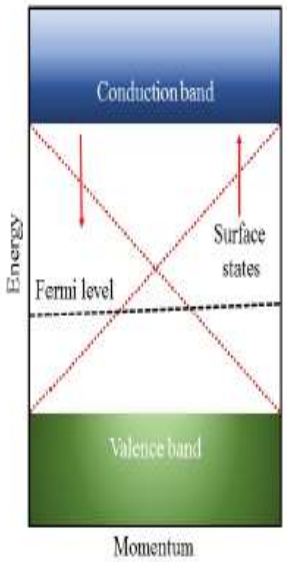

Figure 3
Schematic illustration to show the electronic band structure of a topological insulator in energy vs momentum space.

4. Magnetic Properties of the metal free 2D Systems

Understanding the fundamental difference between vdW 2D and 3D magnetism is informative to understand the driving force of quantum mechanical origin (i.e. exchange interaction) underlying in the ordering of electron spin magnetic moments in an antiferromagnetic system. In this aspect, the mean-field approach of 3D systems does not validate for the length scale of 2D vdW systems, in which the dimensionality (i.e. confinement) effect comes into play. Magnon (i.e., quanta of spin wave) dispersion in such 2D vdW systems attains reduced value compared to that of the 3D counterparts, corresponding to an abrupt onset of magnon density of states (DOS) in 2D vdW systems. For 2D vdW systems without magnetic anisotropy, the spin wave excitation gap reduces. In these materials, any finite nonzero temperatures cause massive magnon excitations and collapsing of the spin order together with the diverging Bose-Einstein statistics of magnons at zero energy. However, a magnon excitation gap opens up and resists the thermal agitations for 2D systems with a uniaxial magnetic anisotropy. In this line, several attempts are performed to create ferromagnetism in nonmagnetic 2D vdW materials since the rise of graphene. One of the mainstream strategies is through introducing vacancies or adding adatoms (i.e. hydrogen and fluorine). Such defect engineering produces local magnetic moments from unpaired electrons, which could be further correlated through conduction electrons in graphene (i.e. itinerant p-magnetism). However, attempts to order these moments in a long-range pattern poses overwhelming challenges in development of the material. Flat band ferromagnetism has been proposed to be realized via extended defects, like zigzag edges of

graphene nanoribbons or grain boundaries of 2D materials. Such defects cause less-dispersed electronic bands that satisfy the huge DOS in a narrow energy scope, leading to the Stoner instability toward a ferromagnetic phase. Remembering the magnetism in 2D vdW systems, the first two reported 2D magnetic atomic crystals are chromium compounds, such as $Cr_2Ge_2Te_6$ (a 2D Heisenberg ferromagnet with small magnetic anisotropy) and CrI_3 (a 2D Ising A-type anti-ferromagnet). Similarly, the magnetic behaviour can be tuned based on the crystal lattice of the 2D vdW systems. However, it is possible to make magnetically ordered chains with finite length and width, so that the finite size ferromagnets behave as spin blocks of super paramagnets with reasonably long spin flipping time, which can provide a practical path toward nanoscale spintronic devices.

5. Two Dimensional van der Waals Heterostructures

In general, these 2D vdW layered materials are usually characterized by extended crystalline planar structures held together by strong in-plane covalent bonds and weak out-of-plane vdW forces. These dangling-bond-free atomic sheets often show extraordinary electronic, topological and magnetic properties in contrast to specific nanostructures that are plagued by dangling bonds and trap states at the surface. These, vdW interactions allow considerable freedom in integrating these 2D layered materials with various nanoscale materials by breaking the vdW bonds to create divers vdW heterostructures without affecting the crystal lattice matching. However, these 2D crystals can be assembled into heterostructures in various methods, like layer-by-layer and interfacial

method. Nevertheless, a large variety of novel prototypes and experiments are going on with these vdW heterostructures, which clearly indicate that these materials are versatile and practical tools for near future experiments and applications.

6. Electronic Properties of vdW heterostructures

In a generalized way, these 2D vdW materials offer great flexibility in terms of tuning their electronic properties. Thus, electronic band-gap engineering can be carried out by changing the number of 2D layers in a given material. However, the rise of vdW materials promotes the possibility of new types of quantum heterostructures with atomically sharp interfaces between the layers of dissimilar 2D vdW materials. Stacking of two or more atomic layers of different vdW materials leads to the rich variety of 2D vdW quantum systems and allows researchers to explore novel and collective electronic, topological and magnetic phenomena at the interfaces. The correlation between electron and spin, phonons, and other electrons can be significantly modulated affecting the charge transport, entropy and total energy in the quantum limit. Moreover, quantum fluctuations are often enhanced and compete with long-range order due to the limited phase-space volume of the heterostructure. As a result, these heterostructures may display emergent electronic phenomena. In other way, the twisting angle between two 2D layers, is an additional degree of freedom in assembling vdW heterostructures. Thus, adjusting the angle between two atomic lattices can result in structures with different electronic properties (i.e. periodic or commensurate structure and incommensurate or quasi-periodic moire

patterns). The important fact is that the physical (i.e. electronic, topological optical and magnetic) properties of such vdW heterostructures often sensitively depend on the interfacial commensurability, thus tuning the twisting angle supports to engineer a large number of combinations of vdW materials. Among the tools for electronic band-structure engineering in vdW heterostruces are the relative alignment between the neighbouring crystals, surface reconstruction, charge transfer, and proximity effects (when one material can borrow the property of another by contact via quantum tunneling or by Coulomb interactions). Thus, the moire structure for graphene on h-BN leads to the formation of secondary Dirac points, commensurate-incommensurate transition in the same system leads to surface reconstruction and gap opening in the electron spectrum, and spin-orbit interaction can be enhanced in graphene by neighbouring TMDC materials.

7. Topological Behaviour and Phase transition in vdW heterosystem

Even more interesting is the specific 2D physics observed in such materials, like, Kosterlitz-Thouless (KT) phase transition in quantum regime, characterized by the emergence of topological order, resulting from the pairing of vortices and antivortices below a critical temperature. Crystals with transition metals in their chemical composition are particularly prone to many-body instabilities such as spin density waves (SDWs), superconductivity and charge density waves (CDWs). Such effects can also be induced by proximity if such 2D vdW crystals are sandwiched with different 2D vdW layer materials. Furthermore, these 2D vdW systems play a specific role in the physics of topological phase

transitions. This transition can be denoted by a topological invariant (Z2) and various phases are detected based on the value of the invariant, like Z2=0 shows trivial phase and Z2=1 shows nontrivial topological phases (i.e. quantum spin hall (QSH) phase). However, it is very rare for a system to have existing long-range order at any finite temperature with a continuous order parameter, implying that even minute thermal fluctuations can destroy order. It is very unique and special that long-range order is possible in 2D vdW systems only at strictly zero temperature (i.e. T=0K). Thus, one can create disorderness in 2D systems by applying an external parameter, like pressure or electric field. In this case, the point at which this 2D system becomes ordered at T=0K is called the quantum critical point, and the transitions are called quantum phase transitions. Thus, it is not the thermal motion that drives the system from order to disorder, but quantum fluctuations in this 2D vdW systems, leading to specific topological phase transitions.

8. Potential Functionalities and outlook of the 2D vdW quantum Systems

The availability of an increasingly broad library of 2D vdW materials with variable electronic properties and the unique ability to integrate into vdW heterostructures enables a new platform for material engineering and device design. The danglingbond-free surface ensures excellent electronic properties and the vdW interlayer interaction allows for considerable flexibility in the systems. The atomically sharp interfaces and highly distinct electronic functions offers a new material prospects and a rich playground for fundamental studies that probe the generation, confinement and transport of charges, exciton, photons and phonons at the limit of single-atom thickness. This empowers the design of a new generation of electronic, energy storage device, catalyst and

spintronics devices with extraordinary performance and unique functionality. Despite the extraordinary potential and considerable progress so far, the challenge of turning these proof of-concept designs into practical technologies should not be understated. Efforts have increased in developing new strategies in understanding the theory and practical implementation of the systems, but current progress is still far from sufficient. The interplay of dimensionality, correlation, charge, orbital character, and topology makes 2D vdW magnetic materials and heterostructures extremely fertile condensed matter systems with a large reservoir of exotic properties. Moreover, another challenge is towards integrating complex 2D vdW heterostructures into functional devices, where a complete understanding of the functional mechanism of these devices is yet to be fully developed. Nonetheless, these new designer materials and unique device structures offer unprecedented opportunities for new applications that represent the future of advance energy storage, catalytic industry, electronics, spintronics and valleytronics.

References:

1. L. Gogoi, W. Gao, P. M. Ajayan and P. Deb, Quantum magnetic phenomena in engineered heterointerface of low-dimensional van der Waals and non-van der Waals materials, *Phys. Chem. Chem. Phys.*, **25** (2023) 1430.
2. B. Keimer and J. Moore, The physics of quantum materials, *Nature Phys*, **13** (2017) 1045.
3. M. Sharma, P. M. Ajayan and P. Deb, Quantum Energy Storage in 2D Heterointerfaces, *Adv. Mater. Interfaces*, **10** (2023) 2202058.
4. D. Basov, R. Averitt, & D. Hsieh, Towards properties on demand in quantum materials, *Nature Mater*, **16** (2017) 1077.
5. Y. Tokura, M. Kawasaki and N. Nagaosa, Emergent functions of quantum materials, *Nature Physics*, **13** (2017) 1056.

INDIAN JOURNAL OF THEORETICAL PHYSICS, VOL 71, NOS. 1 & 2, 2023

Different Aspects of Social Network Analysis and Their Applications

*Kajal De, Shaikh Ibrahim Abdullah

[a]Diamond Harbour Women's University, Kolkata, West Bengal 743368, India, E-mail:

vc.dhwu@gmail.com

[b]Department of Mathematics, School of Sciences, Netaji Subhas Open University, Kolkata, West

Bengal 700064, India, E-mail: skibrahima@gmail.com

Abstract: Social networks are unquestionably a useful and important tool for connecting individuals worldwide. Social Networks are usually represented through graphs, where the vertices of the graphs represent people or groups of people, and the edges represent their connections or relations. Finding famous or important people on social networks is a vital issue. Numerous centrality measures have been introduced over the years to solve this issue. Link prediction is used to find missing or future links between nodes. Here we have given some basic ideas about social networks as an introduction. Different Centrality measures, their applications, Link prediction and their applications are also discussed. We have also discussed the Small World Phenomenon, Homophily, Strength of Ties and their advantages etc. At last, we have concluded it with some future works.

Keywords: Centrality, Small-World Phenomenon, Link Prediction, Homophily, Strength of Ties.

** Prof. P.P. Chattarji Memorial Lecture delivered by Prof. Kajal De, Hon'ble Vice-Chancellor in One Day Seminar on 'Recent Trends of Physics & Mathematics' held on 7 July 2023.*

1. Introduction

Social networks have a long history that dates back to the dawn of humanity. It has always existed since people began helping one another, even if it has largely gone unnoticed. Social change and network theories have been useful in developing Social Network Analysis. It is difficult to trace the beginning of a social structure approach that uses the concept of a "social network" explicitly. However, network thinking originated as a unique approach to social organization in the 1930s. Homans[10] and Emerson are the few researchers who have contributed to developing social change theory. Relationships between network theory and structural analysis have been identified and are now being investigated in disciplines like sociology, social psychology, and anthropology. People are depicted as dots, and connections are shown as lines between the dots when using sociometry to visualize interpersonal connections. This illustration is frequently known as Sociogram[18]. The term "sociometry" was coined by Moreno[14], who also proposed representing social systems as network diagrams, called sociograms, consisting of points and lines. Moreno gave the idea of "sociometry" in his book ”Who Shall Survive”[14]. In 1938 Moreno and Jennings were the first to introduce modern social network analysis.

Social networks are collections of people or groups of people related to one another. The mode could be offline or online. These offline networks are common: family members establish a network (family network), students of a school form a student network, some farmers in a village form a farmer network, and doctors in a city form a doctor network. Millions of people use smartphones, and they find it quite comfortable to connect with one another and share information via social media. Online social networks like Twitter, Facebook, and LinkedIn have recently experienced tremendous

growth in popularity among people. Throughout the social network, relationships exist between people, co-workers, businesses, etc. So, it is a platform for advertising goods, sharing information, etc. Social networks have changed dramatically since the start of this century. In the current era of connectedness, most businesses supplement their traditional marketing plans with digital ones that heavily utilize social media platforms. Social media has grown in popularity, and as a result, it has become a crucial component of organizations' advertising and marketing strategies.

2. Centrality Measures

In social networks, prominent nodes are identified using centrality metrics. The fundamental problem of social networks is finding the central or influential node. A node's Centrality in a social network indicates the popularity of the node. In a bank, the branch manager can be assumed central among all the employees of the branch. Similarly, in a school, the head teacher can be assumed more central among all the teachers of the school. Due to high applicability, research is going on about social networks and different centrality measures. The concept of centrality measure was first introduced by Bavelas[5] in 1948.

2.1. Different Centrality Measures

Numerous centrality measures have been developed over the years to find influential nodes. Some of the important centrality measures are discussed below:

2.1.1. Degree Centrality

Shaw[17] first introduced the idea of Degree Centrality in 1954. The first mathematical model for Centrality was developed by Freeman[7] in 1978.

The Degree Centrality of node u is defined as CD(u) = d(u), where d(u) is the degree of node u.

For normalization, Degree Centrality is defined as CD′(u) = d(u) (n−1) , where n is the no. of nodes of the network[6].

It is used for finding the location of emergency services like hospitals, fire brigades, police stations etc.

Let us consider the network given in Figure 1:

Clearly, in Figure 1, CD(5) = 5.

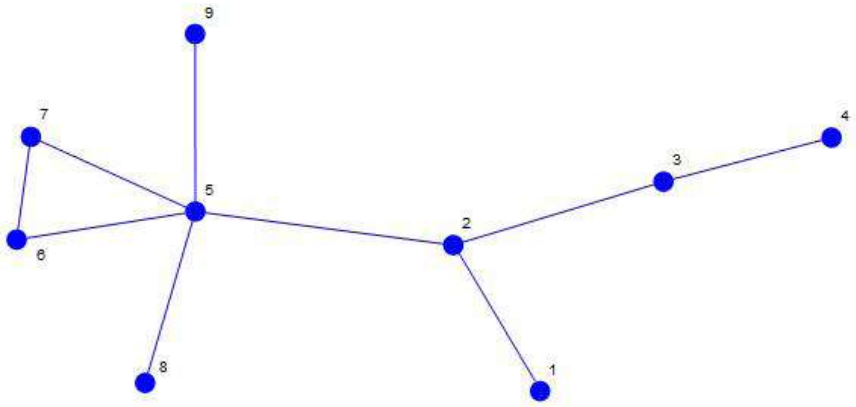

Figure 1

A network consisting of nine nodes.

2.1.2. Closeness Centrality

The idea of the Closeness Centrality measure was introduced by Bavelas[5] in 1948 and defined in 1966 by Sabidussi[16]. Freeman[7] developed a mathematical model for Closeness Centrality in 1978.

The Closeness Centrality of a node v in a network is defined as, $C_C(v) = \frac{1}{\sum_{u \epsilon V} d(u,v)}$, where V is the set of nodes in the network.

For normalization, Closeness Centrality is defined as, $C_{C'}(v) = \frac{n-1}{\sum_{u \epsilon V} d(u,v)}$, where n is the number of nodes of the network[6].

It is used for finding the location of shopping malls, markets etc. In Figure 1, $C_{C'}(5) = 0.67$.

2.1.3. Eccentric Centrality

Hage and Harary[9] developed the idea of eccentricity in social networks in 1995. The Eccentric Centrality of a node u in a network is defined as, $C_{EC}(u) = \frac{1}{max_{v \in N} d(u,v)}$, where N be the set of nodes of the network[6].

In Figure 1, , $C_{EC}(5) = 0.33$.

2.1.4. Betweenness Centrality

Shaw[17] first gave the concept of centrality measures based on betweenness in 1954. Freeman[7] gave the first formal definition of Betweenness Centrality in 1978. The Betweenness Centrality C_B of a node v is defined as,

$C_{B(v)} = \sum_{p,q \in N: p \neq v \neq q} \frac{\sigma_{pq}(v)}{\sigma_{pq}}$, where $\sigma_{pq}(v)$ is the no. of shortest paths between p and q containing v, and σ_{pq} is the no. of shortest paths between p and q, and N is the set of nodes.

It is used to find a location from which signals can be controlled in a communication network.

In Figure 1, $C_B(5)$ = 21.

2.1.5. K-shell Centrality

The k-shell decomposition method was first developed by Kitsak et al.[11] in 2010.

In this method, at first, all the nodes of degree 1 are removed. After this, there may be some pendant nodes. So, this process has to be continued until there are no pendant nodes. The eliminated nodes are allocated to 1-shell. Similarly, all the nodes of degree 2 are eliminated, and after this process, if there is any node of degree less than or equal to 2, then they have to be removed. This process has to be continued until there is no node of degree less than or equal to 2. These nodes are allocated to 2-shell. This procedure must be repeated until all nodes are exhausted, i.e., each node is assigned to any of the k-shells. This centrality metric is used to find super-spreader nodes in a network.

In Figure 1, $C_{KS}(5) = 2$.

2.1.6. Neighborhood Coreness Centrality

This centrality measure was first introduced by Bae and Kim[4] in 2014.

The Neighborhood Coreness Centrality of a node in a network is given as,

$C_{NC}(v) = \sum_{u \in N(v)} ks(u)$, where $N(v)$ is the set of neighbors of v and $ks(u)$ is the k-shell value of node u.

The Extended Neighborhood Coreness Centrality of node v is defined as,

$$C_{NC'(v)} = \sum_{u \in N(v)} C_{NC}(u).$$

It is used to measure the spreading of contagious diseases.

In Figure 1, $C_{NC}(5) = 7$.

2.2. Real-Life Applications of Centrality Measures

- Centrality measures are used to measure the spreading of the menace of society like alcohol and drug consumption etc.
- Centrality metrics are used to find the location of markets, police stations etc.
- It is used to find masterminds in terrorist activities and cyber crimes.
- In communication networks, it is used to find the amount of communication passing through a particular node.
- It is used to measure traffic congestion in road networks.
- It has huge applications in transportation problems.
- Centrality measures are applied for marketing purposes to make something viral in a very quick time.
- It is used in the structure of molecules or chemical compounds.
- Centrality measure, like Page-rank centrality, is used to find the importance of online pages.
- Centrality metrics are used in biological networks to find the lethality of protein in the protein interaction network.
- Centrality metric, like Leverage Centrality, is used in the human brain network.

3. Small-World Phenomenon

At Harvard University in the late 1960s, Stanley Milgram[13] conducted a fascinating experiment. He distributed several letters to the people of Nebraska, who were chosen randomly. The letters were addressed

to a stockbroker acquaintance of his in Boston, Massachusetts. Nebraska, in his opinion, was the farthest away from Boston. He instructed that the letters should be handed from person to person to reach their intended recipient (the stockbroker) and that they could only be passed to someone the passer knew by first name. Their best strategy was to pass their letter to someone whom they felt was nearer to the stockbroker in some social sense: perhaps someone they knew in the financial industry or a friend in Massachusetts. A reasonable number of Milgram's letters did eventually reach their destination, and Milgram found that it only required six steps on average for a letter to go from Nebraska to Boston. Thus he conjectured that a similar separation might characterize the relationship between any two people in the entire world. This phenomenon has been labelled "six degrees of separation".

The "six degrees of separation" has a wide range of applications, but it is sometimes criticised. Later, it was found that the number of degrees of separation between Albert Einstein and Alexander the Great is almost certainly greater than 30, and this network does not have small-world properties. Similarly, it was noticed that if two people went to the same college ten years apart from one another, it is unlikely that they have acquaintances in common among the student body.[15]

It is evident from "Six Degrees of Separation" that any two persons in the world are only a few steps apart, regardless of how far apart they are. This leads to the concept of the Small-World Phenomenon. A very important finding of social networks is the small world phenomenon. The majority of the nodes in a small-world network are not neighbours of one another, but the neighbours of any particular node are most likely to be neighbours of one another. As a result, the majority of nearby nodes are only a few steps

or feet away from every other node. Cliques and nearcliques, or sub-networks with connections between virtually any two nodes within them, are common in small-world networks. The simplest explanation for the small world effect uses the idea of a random graph.

Let there is n number of people in the world, and on average, they each have z acquaintances. This implies that there are $\frac{1}{2}nz$ connections between people in the entire population. The number z is called the coordination number of the network. A very simple model of a social network can be made by taking n nodes and drawing $\frac{1}{2}nz$ links between randomly chosen pairs to represent these connections. Such a network is called a random graph. It is easy to see that a random graph shows the small-world effect.

If a person A on such a graph has z neighbours, and each of A's neighbors also has z neighbours, then A has about z^2 second neighbours. Extending this argument, A also has z^3 third neighbours, z^4 fourth neighbours and so on. Most people have between a hundred and a thousand acquaintances, so z^4 is already between about 10^8 and 10^{12}, which is comparable with the population of the world. In general, the number D of degrees of separation, which we need to consider in order to reach all n people in the network, is given by $z^D = n$, which implies that D = $\frac{logn}{logz}$. Since $logn$ increases only slowly with n, it allows the number of degrees to be quite small, even in very large systems.[15]

Figure 2

Small World Phenomenon[3].

3.1. Applications of Small-World Phenomenon

Small-World Phenomenon has many real-life applications. Some of them are discussed below:

- Social networking sites use the small world theory to suggest relationships and boost networking.
- The small-world phenomenon is used to stop the outbreak of contagious diseases.
- It is used to find influential people and increase the distribution of ideas or products.
- Transportation networks can be optimized by considering the small world phenomenon to improve connectivity and efficiency.
- Studying the small world phenomenon can help improve the design of computer networks, enhancing data transmission and connectivity.

- Online recommendation systems employ the small world phenomenon to suggest relevant content or products based on the connections and preferences of similar users.
- The small-world phenomenon is very helpful for any agitation to be successful.

4. Link Prediction

Link prediction refers to the task of predicting the likelihood or probability of a future or missing link between nodes in a network. It involves analyzing the existing network structure and its properties to infer potential connections that are not currently present. Link prediction techniques utilize various algorithms and measures to estimate the likelihood of forming a connection between two nodes based on factors such as shared neighbours, structural similarity, or network dynamics. The goal of link prediction is to gain insights into the evolving nature of networks, identify potential future connections, and improve network-based predictions, recommendations, or decision-making processes.

4.1. AUC Method for Link Prediction

Let $G(V, E)$ be an undirected simple network, where V is the set of nodes and E is the set of links. Let U denotes the universal set containing all $\frac{|V|(|V|-1)}{2}$ 2 possible links, where $|V|$ denotes the number of elements in set V. Then, the set of nonexistent links is $U - E$. We assume there are some missing links (or the links that will appear in the future) in the set $U - E$ and the task of link prediction is to find out these links. E is randomly divided into two parts: the training set, E^T, is treated as known information, while the probe set, E^P, is used for testing, and no information in this set is

allowed to be used for prediction. Clearly, $E^T \cup E^P = E$ and $E^T \cap E^P = \phi$. A link prediction algorithm provides each non-observed link, say $(x, y) \in U - E^T$, a score, s_{xy} to quantify its existence likelihood. The *AUC* value can be interpreted as the probability that a randomly chosen probe link (i.e., a link in E^P) is given a higher score than a randomly chosen non-existent link (i.e., a link in $U - E$). Then, at each time, we randomly pick a missing link and a non-existent link to compare their scores; if among n independent comparisons, there are n' times the missing link has a higher score and n'' times they have the same score, the *AUC* value is, $AUC = \frac{n' + 0.5n''}{n}$ [12].

4.2. Applications of Link Prediction

Some applications of Link Prediction are discussed below:

- Link prediction forecasts future interactions and reveals potential social relationships between persons.
- On the basis of users' past searches, link prediction techniques are used to suggest relevant things or products to them.
- Link prediction examines the relationships and connections inside a network to find suspicious patterns or potentially fraudulent actions like spam emails, etc.
- Link prediction aids in forming effective teams or collaborations by predicting potential connections and identifying individuals with complementary skills or expertise.
- By detecting possible interactions or links between individuals in a network, link prediction can help predict the spread of diseases.

- By predicting appropriate links or connections between online sites or documents, link prediction can enhance search engine results.
- Link prediction techniques help detect and prevent potential security threats by identifying suspicious or unauthorized connections in a network.

5. Homophily

The tendency for people to connect with and associate with those who are similar to them in a variety of ways is known as homophily in society. In social networks, homophily is the tendency for people to connect with or collaborate with others who have similar traits, features, or interests. It is the principle that individuals are more likely to connect and interact with people who are similar to themselves. Homophily can manifest across various dimensions, such as demographics (age, gender, ethnicity), socioeconomic status, interests, beliefs, attitudes, and values. It has significant effects on the dynamics and structure of social networks, influencing the establishment of communities or groupings of people who have similar traits. Homophily can affect social influence, consolidate existing ideas, and support both potential discrimination and social cohesion.

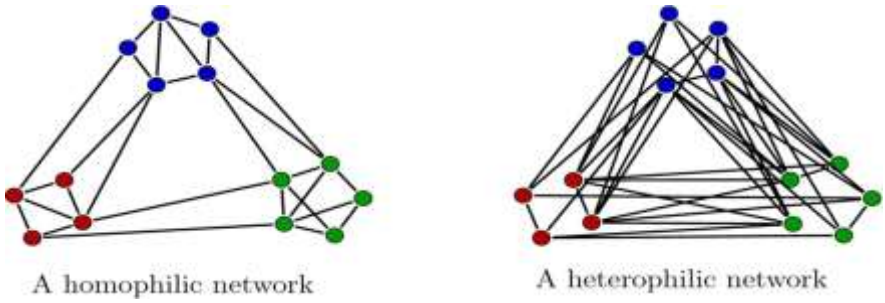

Figure 3

Homophilic and Heterophilic Network[1].

5.1. Advantages of Homophily

- Homophily promotes social cohesion by fostering connections and interactions among individuals who share similar attributes or interests.
- Homophily allows for a shared understanding and common ground among individuals, leading to easier communication and strong bonds.
- Homophily can contribute to trust and reliability within social relationships, as individuals may perceive others with similar characteristics as more trustworthy.
- It can help preserve and pass on cultural traditions, practices, and values within specific communities or social groups.
- Homophily fosters supportive networks where individuals can find empathy, validation, and emotional support from like-minded peers.
- Homophily enhances the sharing of information and knowledge among individuals with similar interests or experiences, exchanging valuable insights and resources.
- Homophily promotes efficient communication by reducing misunderstandings and facilitating shared language or cultural references.

5.2. Disadvantages of Homophily

- Homophily can lead to a lack of diversity in social networks or communities as individuals tend to associate and bond with others similar to them regarding beliefs, values, interests, and backgrounds.

- People may be less likely to encounter divergent points of view or be exposed to creative concepts when interacting with those who share their perspectives, which may hinder personal development and innovation.

- Networks characterized by homophily may restrict access to resources such as job opportunities, information, and support systems. This can create inequalities and limit social mobility for individuals not part of the dominant groups within those networks.

- Homophily can reinforce existing social inequalities by promoting advantages for certain groups while excluding or marginalizing others who do not fit the dominant social norms within those networks.

- Interacting with people who have different backgrounds and perspectives provides valuable learning opportunities. Homophily limits these opportunities, hindering personal and intellectual growth.

6. Strength of Ties

6.1. Strong Ties and Weak Ties

Ties in social networks refer to the connections or relationships between individuals or entities within a network. These ties represent the links between nodes, indicating various forms of social interactions and connections. Sociologist Mark Granovetter[8] introduced the concept of strong and weak ties in his influential work on social networks. Strong ties refer to close, intimate, and emotionally significant relationships between individuals in a social network. These ties typically involve frequent intense interactions, trust, and mutual support. Examples of strong ties include family members, close friends, and romantic partners. Strong ties often

involve shared experiences, mutual obligations, and a high emotional connection. They provide a sense of belonging and emotional support and are crucial for social and psychological well-being.

On the other hand, weak ties represent more casual and less intimate connections between individuals in a social network. These ties involve infrequent interactions, limited shared experiences, and lower emotional intensity than strong ties. Weak ties often exist between acquaintances, distant friends, or individuals who share a limited interaction context. While weak ties may not offer the same level of emotional support as strong ties, they provide access to diverse information, resources, and opportunities. Weak ties are crucial in bridging different social circles, facilitating information diffusion, and offering novel perspectives or connections outside one's immediate social group.

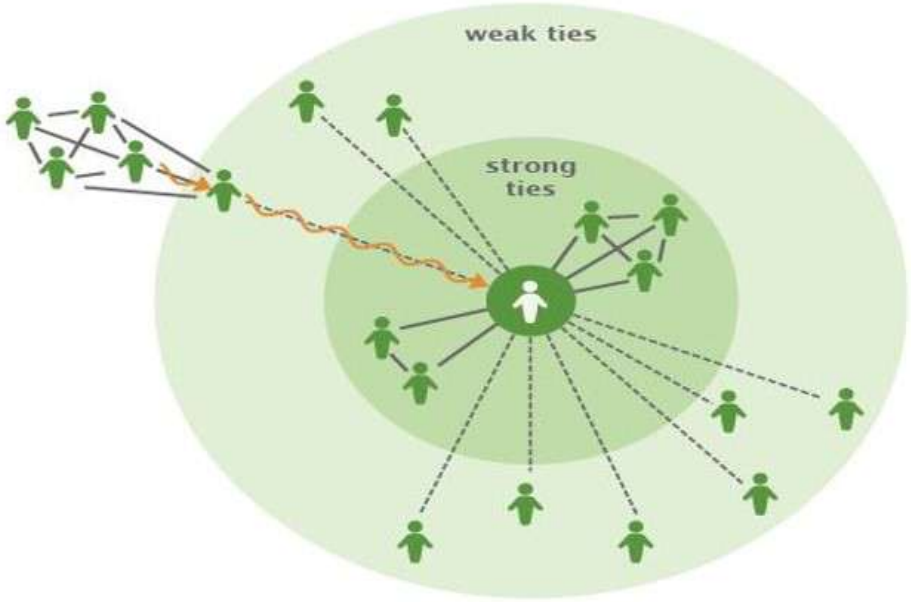

Figure 4

Strong Ties and Weak Ties[2].

6.2. Positive and Negative Ties

Positive ties, also known as positive relationships or affiliations, refer to connections in a social network characterized by positive emotions, cooperation, and mutual support. These ties are marked by trust, empathy, and a sense of mutual benefit or shared goals. Positive ties can encompass various types of relationships, such as friendships, supportive family connections, and cooperative professional relationships. Positive ties contribute to social well-being and positive interpersonal experiences within a network.

Negative ties, also referred to as negative relationships or conflicts, represent connections in a social network that are characterized by negative emotions, disagreement, and hostility. These ties involve animosity, tension, or competition between individuals. Negative ties can arise due to personal differences, conflicting interests, or negative experiences in the past. Examples of negative ties include interpersonal conflicts, rivalries, or strained relationships. Negative ties can harm individual well-being, social cohesion, and overall network dynamics. Managing and resolving negative ties is important for maintaining a healthy social network and fostering positive interactions among its members.

6.3. Why Are Weak Ties Sometimes Considered Better Than Strong Ties?

It is important to note that weak ties are not universally "better" than strong ties. However, weak ties are sometimes considered better due to having some advantages over strong ties. Here are some benefits of weak ties:

- Weak ties provide access to diverse information and perspectives outside of one's immediate social circle.
- Weak ties increase the chances of encountering unexpected opportunities, such as new job prospects or collaborations.
- Weak ties act as bridges between disconnected social circles, promoting social integration and cross-cultural understanding.
- Weak ties offer alternative viewpoints and stimulate creative thinking by introducing different ideas and perspectives.
- Weak ties expand one's network beyond close friends and family, connecting with individuals from different social groups and communities.
- Weak ties expose individuals to a wider range of experiences and perspectives, enabling them to adapt more effectively to changing circumstances and environments.
- Weak ties can provide opportunities for marginalized individuals to improve their social circumstances.

7. Conclusion

A social network, in general, consists of a collection of nodes or actors and a relationship, connection, or links between nodes. All people might not behave or have the same character as one another, and their connections might not have the same strength in the network. Applications for centrality metrics can be found in a wide range of fields, including sociology, psychology, economics, anthropology, biology, terrorism, traffic, neuroscience, business, etc. Different centrality measures have been

developed to find important nodes in the network and research is going on to find better centrality metrics as far as accuracy and time complexity is concerned. Different aspects of Social Network Analysis, like, Link Prediction, Small-World Phenomenon etc., have huge real-life applications. Investigating more about fuzzy social network analysis is an open issue. So in the future, research can be done on fuzzy social networks to explore how actors behave there. New centrality measures can be developed for the marketing strategy to make advertisements viral in less time.

References

1. Examples of homophilic and heterophilic networks. In both cases three... | Download Scientific Diagram.
2. LinkedIn on the Power of Weak Ties - Implications for Coworking Freelancers - Small Business Labs.
3. The Six Degrees of Separation theory - HackerEarth Blog.
4. J. Bae and S. Kim. Identifying and ranking influential spreaders in complex networks by neighborhood coreness. Physica A: Statistical Mechanics and its Applications, **395**:549–559, 2014.
5. A. Bavelas. A mathematical model for group structures. Human organization, 7(3):**16–30**, 1948.
6. K. Das, S. Samanta, and M. Pal. Study on centrality measures in social networks: a survey. Social network analysis and mining, 8:**1–11**, 2018.
7. L. C. Freeman et al. Centrality in social networks: Conceptual clarification. Social network: critical concepts in sociology. Londres: Routledge, 1:**238–263**, 2002.
8. M. Granovetter. Thestarch of weak ties. American Journal of Sociology, 78(6):**1360–1380**, 1973.

9. P. Hage and F. Harary. Eccentricity and centrality in networks. Social networks, 17(1) : **57–63**, 1995.

10. G. C. Homans. Social behavior as exchange. American journal of sociology, 63(6): **597–606**, 1958.

11. M. Kitsak, L. K. Gallos, S. Havlin, F. Liljeros, L. Muchnik, H. E. Stanley, and H. A. Makse. Identification of influential spreaders in complex networks. Nature physics, 6(11) : **888–893**, 2010.

12. L. Lü and T. Zhou. Link prediction in complex networks: A survey. Physica A: statistical mechanics and its applications, 390(6):**1150–1170**, 2011.

13. S. Milgram. The small world problem. Psychology today, 2(1):**60–67**, 1967.

14. J. Moreno. Who shall survive? nueva york, 1934.

15. M. E. Newman. Models of the small world. Journal of Statistical Physics, 101 : **819–841**, 2000.

16. G. Sabidussi. The centrality index of a graph. Psychometrika, 31(4):**581–603**, 1966.

17. M. E. Shaw. Group structure and the behavior of individuals in small groups. The Journal of psychology, 38(1):**139–149**, 1954.

18. S.Wasserman and K. Faust. Social network analysis: Methods and applications. 1994.

INDIAN JOURNAL OF THEORETICAL PHYSICS, VOL 71, NOS. 1 & 2, 2023

Application of MATLAB in the analysis of High Impedance Fault

Indranil Bhattacharaya*, Partha Sarathi Majumdar

Dept. of Physics, A.P.C College,New Barrackpore, Kolkata-700131, WB.

Pratyusha Biswas Deb

Department of Electrical Engineering, Narula Institute of Technology, Agarpara, Kol-700109, WB

Soumya Das

Project Engineer, Larsen & Tubro Limited, Jeddah, Saudi Arabia.

S. Dorendrajit Singh

Department of Physics, Manipur University, Canchipur, West Imphal, 795003, Manipur

Abstract : There is problem in the detection of high impedance fault using conventional technique. This problem can be overcome by using fast Fourier-Transform technique considered in the present paper.

KEYWORDS: High Impedance Fault - *HIF*, Fast Fourier Transform - *FFT*, Power System Measuring Units,

*Corresponding Author : indranil@apccollege.ac.in, 09434348865

1. INTRODUCTION

A 3-phase AC power system operating under normal condition has a standard magnitude of both current and voltage which is equally distributed across each phase, when a fault occurs on the system a high short circuit[1] current flows in system causing unbalanced voltage and reduces the effective impedance of the system which destroys and damages the protective equipment connected in the system. The High Impedance Fault (HIF) current random behavior and its low magnitude cause difficulties for a reliable detection by traditional protection methods. Therefore, the hazards for grid devices and people's safety associated with $HIFs$ motivate better at suitable detection techniques. Short-circuit currents are harmful for two reasons- the first is that even a short-time flow of heavy current will overheat the equipment, the second is that the flow of short-circuit currents through the current carrying parts produces forces of electrodynamic[2] interaction which may destroy or damage the equipment. This is why all the elements of any electrical installation are designed and selected for a thermal and a dynamic stability is sufficient to withstand the largest possible flow of short circuit current that may occur in the given installation. The severest conditions in service are those of the switching devices during a short circuit. These devices are circuit breakers[3] and the fuses, whose function is to interrupt the fault current within a short period or time (0.05 - 0.3 second) and thereby switch out the faulty section. The power system equipment like relay, circuit breaker ad others do not work well due to the presents of harmonics so the detection of fault current and over voltage is failed and as a whole a fault occurs in total system. So, short circuit current

analysis and harmonics analysis with quick function is most important task for the protection function. If the fault current analysis is done quickly and accurately, the protective equipment can do their operation within the time.

Therefore, HIF occurrence is a major challenge for distribution networks. Also, the electric arc leads to distinctive features on the fault current waveform as well as a peculiar frequency spectrum. Consequently, several types of research stimulate the use of harmonic content to detect HIF faults. Thus, this paper presents a study of a variant of the FT, called Fast Fourier Transform[4] (FFT)".

In this paper, short circuit current analysis and harmonics analysis are done with the Fast Fourier transform (FFT). So, the fault current FFT analysis is done for protection operation of total electrical system within the time for completing the fault clearing operation within the 'critical fault clearing time' to maintain the steady state stability.

2. SYSTEM MODELLING

This section presents the methodology proposed in this paper concerning implementing an electrical system, the $HIFs$, and other events related to electrical transmission and distribution systems, which are required to prove the method's robustness. Therefore, the simulations were carried out according to the following subsections.

2.1 High Impedance Faults

High Impedance Faults ($HIFs$) on distribution feeders are defined as abnormal electrical conditions that cannot be detected and cleared by conventional protection schemes, due to their low fault current. Faults

resulting from neighboring objects making prolonged contact with the energized line can endanger human life, potentially causing severe electrical burns, electrocution or fires. Additionally, the arcing associated with HIF may also lead to serious damage to the power system. HIF occurs when the energized overhead distribution feeder conductors have undesired physical contact with a quasi-insulating object nearby, such as asphalt road, gravel or tree limbs. The current from this type of fault may be too small to be detected by conventional protection devices. Therefore, the downed energized conductor may become a potential hazard to public safety. Furthermore, arcing is often associated with these faults.

HIF typically caused by broken conductor in touch with ground and other surfaces but still connected to source, intermitted contact with tree limbs or other objects, contaminated or falling equipment etc.

2.2 Test System

All developed countries depend upon electrical energy for industrial, commercial, agricultural, domestic and social purposes. Therefore, the basic infrastructure, that is, generating stations and transmission and distribution lines have become a crucial part of modern socio-industrial landscape. So, we choose $\boldsymbol{IEEE-9}$ BUS System for standard calculation and simulation, where 3 generators are connected with 3 Transformers, then power is transmitted over transmission line and is distributed in 3 load buses and 1bus specified as swing bus. It is a specially designed grid system which has 9 buses arranged in a specific pattern in accordance to $\boldsymbol{IEEE}$ norms. Simulation will be applied on this test system

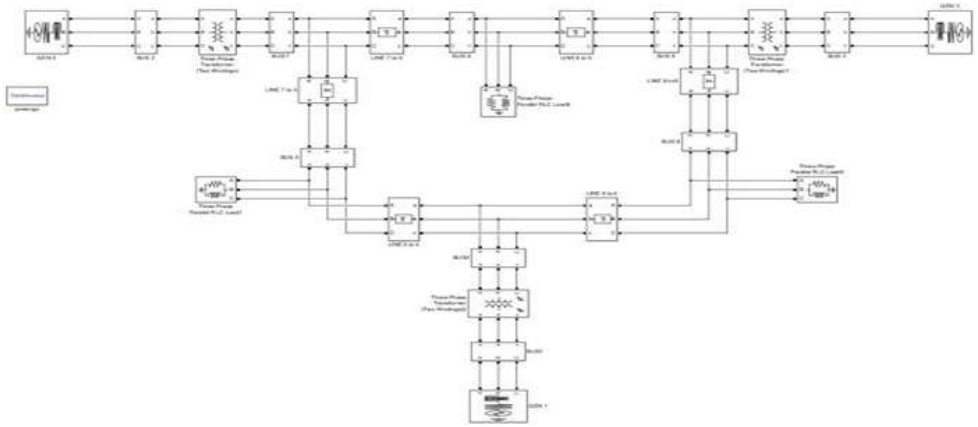

Figure 1

IEEE 9-Bus standard system

2.3 Simulation Software

MATLAB is a programming and numeric computing platform software used to analyze data, develop algorithms, and creates models and design systems and simulation. In this paper, we use MATLAB 2014a[5] software to create the total 9-Bus system Simulink model and total experiments have been done.

3. PROPOSED METHODOLOGY

The proposed *HIF* detection method in this study aims to identify *HIF* by monitoring the phase current, using only the substation as an observable point. By the analysis of the phase current spectrograms and the state of the art. In the case of *HIF* detection, the signal processing technique is popular and this gives most correct result.

3.1 Fourier Transform

Frequency domain techniques can be used for obtaining the signals harmonic content. Since the *FT* can extract information about the magnitudes of the various signal frequencies and because it is widely used

in the protection systems of Electric Power Systems (EPS), it is used in the methodology proposed by this work. For defining the Fourier transform of an integral function.

$$\hat{f}(\xi) = \int_{-\infty}^{\infty} f(x)\, e^{-2\pi i x \xi}\, dx, \quad \forall\, \xi \in \mathbb{R}. \qquad \ldots(1)$$

The Fourier transform is denoted here by adding a circumflex to the symbol of the function. When the independent variable x represents time, the transform variable ξ represents the frequency.

Under suitable conditions *f* is determined by $\hat{f}$ via the inverse transform:

$$f(x) = \int_{-\infty}^{\infty} \hat{f}(\xi)\, e^{2\pi i x \xi}\, d\xi, \quad \forall\, x \in \mathbb{R}. \qquad \ldots (2)$$

That is known as the Fourier inversion theorem[6].

In order to observe certain signal frequencies, the size, and consequently the number of samples in each window, can be changed, thus modifying the frequency resolution Δf of the signal with a sampling frequency fs and N is number of samples.

$$\Delta f = \frac{fs}{N} \qquad \ldots (3)$$

Inter-harmonics are commonly found in HIF current waveforms, because they are associated with the random length variation of the electric arc during fault situations. In this condition, the larger the amplitude of the variation, the larger the number of inter-harmonic frequencies.

There are some processes of FT such as Continuous Fourier Transform (CFT), Discrete Fourier transforms (DFT), Discrete Time Fourier Transform ($DTFT$), Fast Fourier transforms (FFT), Short Time Fourier transforms ($STFT$).

3.2 Discrete Fourier Transform

In mathematics, the discrete Fourier transform (DFT)converts a finite sequence of equally-spaced samples of a function into a same-length sequence of equally-spaced samples of the discrete-time Fourier transform ($DTFT$), which is a complex-valued function of frequency. The interval at which the $DTFT$ is sampled is the reciprocal of the duration of the input sequence. An inverse DFT is a Fourier series, using the $DTFT$ samples as coefficients of complex sinusoids at the corresponding $DTFT$ frequencies.

The discrete Fourier transform transforms a sequence of N complex numbers into another sequence of complex numbers,

$$\{\mathbf{x_n}\} := x_0, x_1, \ldots, x_{N-1} \quad \ldots \quad (4)$$

$\{\mathbf{X_k}\} := X_0, X_1, \ldots, X_{N-1}$, it is defined by

$$\begin{aligned} X_k &= \sum_{n=0}^{N-1} x_n \cdot e^{-\frac{i2\pi}{N}kn} \\ &= \sum_{n=0}^{N-1} x_n \cdot \left[\cos\left(\frac{2\pi}{N}kn\right) - i \cdot \sin\left(\frac{2\pi}{N}kn\right)\right], \end{aligned}$$

where the last expression follows from the first one by Euler's formula. The transform is sometimes denoted by the symbol F, as in

$F(x)$ or $X = F\{x\}$ or Fx. The discrete Fourier transform is an invertible. The inverse transform is given by:

$$x_n = \frac{1}{N} \sum_{k=0}^{N-1} X_k \cdot e^{i\frac{2\pi}{N}kn}$$

The DFT has seen wide usage across a large number of fields. All applications of the DFT depend crucially on the availability of a fast algorithm to compute discrete Fourier transforms and their inverses, a fast Fourier transform (FFT).

3.3 Fast Fourier Transform

A fast Fourier transform (FFT)[7] is an algorithm that computes the discrete Fourier transform (DFT) of a sequence, or its inverse ($IDFT$). Fourier analysis converts a signal from its original domain (often time or space) to a representation in the frequency domain and vice versa. The DFT is obtained by decomposing a sequence of values into components of different frequencies. An FFT rapidly computes such transformations by factorizing the DFT matrix into a product of sparse (mostly zero) factors. As a result, it manages to reduce the complexity of computing the DFT from $O(N^2)$, which arises if one simply applies the definition of DFT, to $O(N\log N)$, where N is the data size and $N = 2$ here. The difference in speed can be enormous, especially for long data sets where N may be in the thousands or millions. In the presence of round-off error, many FFT algorithms are much more accurate than evaluating the DFT definition directly or indirectly. Because $\lim_{N\to\infty} \frac{log_2 N}{N} = 0$ it is a typical fast algorithm. Fast algorithms of this type of recursive halving are very typical in scientific computing. So, FFT is faster than DFT.

Applying DFT using a FFT algorithm reduces the time complexity required in practical applications. Thus, this work uses the FFT calculation in specific signal windows, making it possible to obtain values in the magnitude of all frequencies during the entire fault time. Therefore, the way the FFT is calculated for a discrete signal.

4. SOLUTION METHOD

Total work is done with the following stage by stage:

- First, $IEEE\ 9-BUS$ standard system is created with $MATLAB$ Simulink model with standard value and run it in steady state

performance using $MATLAB$ 2014 a software.

- Stage 2, in the system HIF is created at some location and done the simulation.
- Stage 3, after simulation we collected all data of faults.
- Stage 4, at last with creating the faults the FFT analysis is applied and all data are collected.

5. RESULT AND SOLUTION

Transmission line protection is an important issue in power system because 85-87% of power system faults are occurring in transmission line. This dissertation work gives technique to classify the different faults on transmission line for quick and reliable operation of protection schemes.

Transmission line faults are of mainly five types: L-G, L-L, L-L-G, L-L-L and L-L-L-G. But the effect of L-L-L and L- L-L-G faults is same. So, here we are considering only L-L- L fault. In all four different faults are classified after faulty condition is detected in the system. In order to detect the existence of $HIFs$, we propose to use FFT. The traditional approach uses FFT to detect HIF current of the event in a large size frame. By doing this, one could miss the existence of the HIF in the transient state where the duration of occurrence is very short.

All the fault cases are discussed in the results initially all the types of faults are made near bus 2 and bus 7. The cases of faults made at a distance of 25km are considered for the result analysis. Here, take the values and graphs of FFT for every type of HIF. By the result, it is observed that how faults are detected very quickly with applying the FFT signal processing technique.

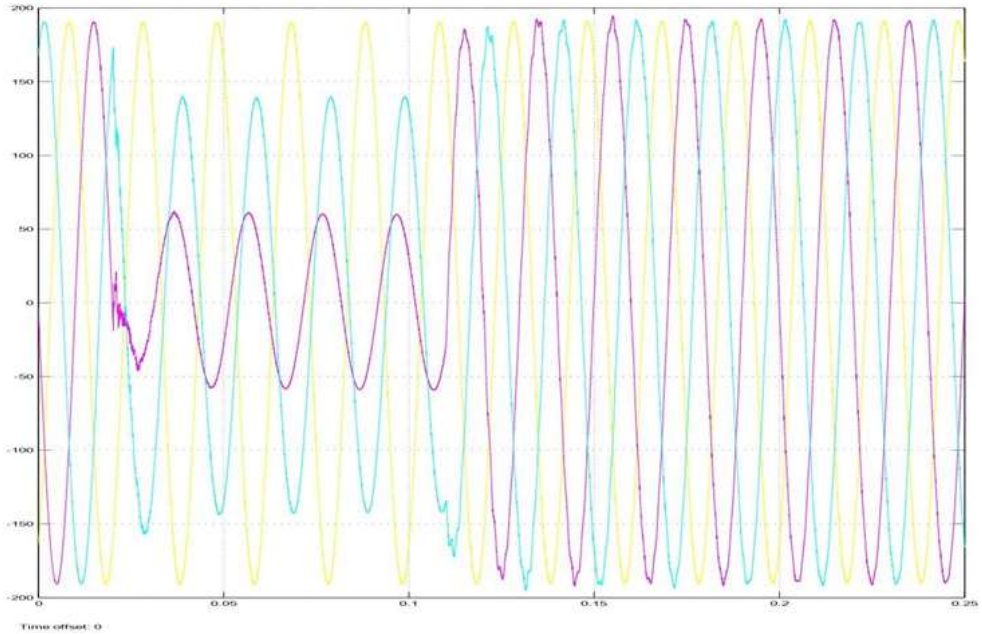

Figure 2

Fault current of 3 phase for line-to-line fault

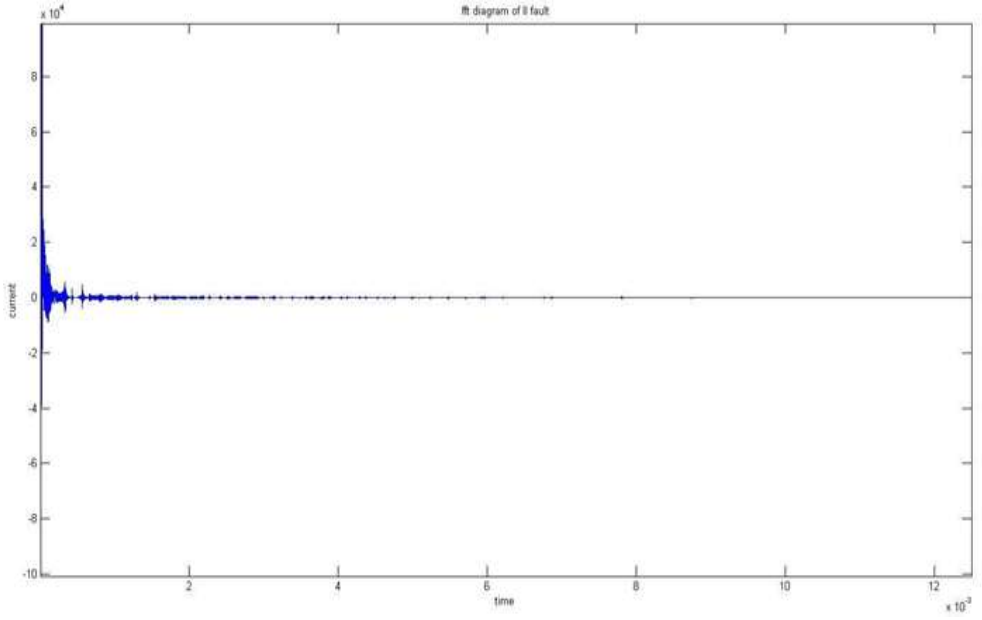

Figure 3

Line to line fault current FFT analysis

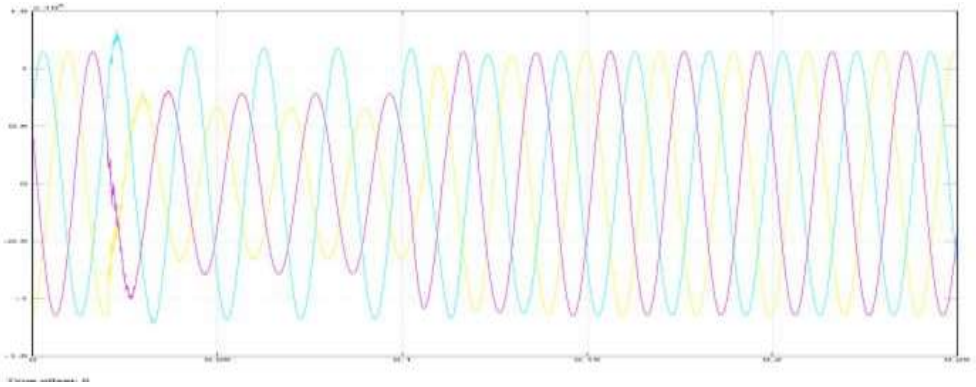

Figure 4
Fault current of 3 phase for line to line to ground fault

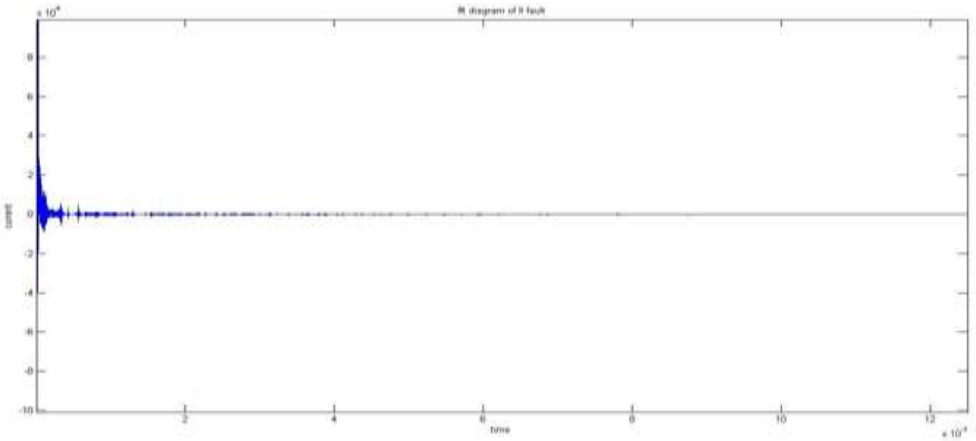

Figure 5
Line to line fault current FFT analysis

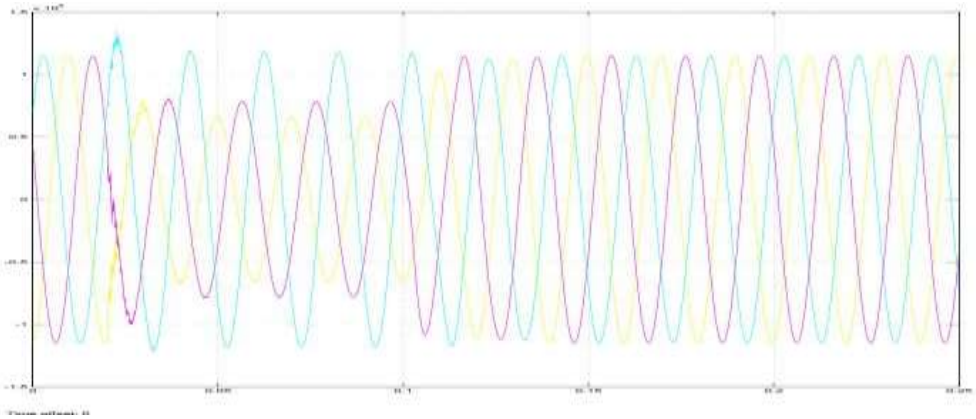

Figure 6
Fault current of 3 phase for line to ground fault

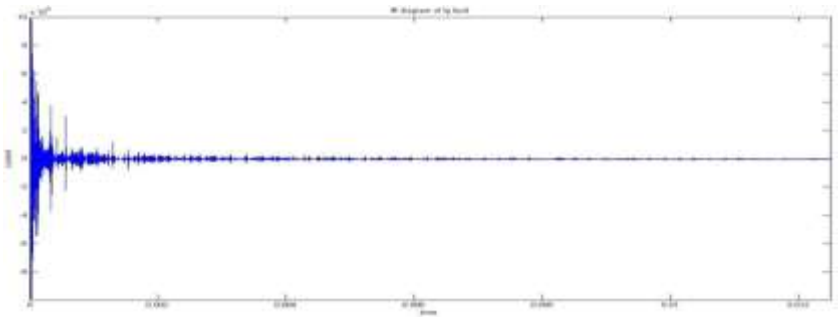

Figure 7
Line to ground fault current FFT analysis

It is observed that during the HIF, the value of current decreases from the nominal value, as shown in the diagram. When the Fault is removed, the system attends its normal value. Whereas for the voltages, at the time of occurrence of the fault, there is large surges at that instant while the nature of the waveform is retained.

If a HIF detection method has only one sensor at the substation, it would be necessary to use the low-frequency content, which can be done either by harmonics or inter- harmonics. On the other hand, if the sensor is nearby the HIF location, it would be possible to use the current higher frequencies energy amplitude and variation for HIF detection.

In future, the protection system provided for the system should have fast response. According to this analysis, fast fault clearing and load shedding methodologies can be adopted for system stability and also be applied for finding fault location.

For future studies, the method can be applied in other test systems with topology variations like intelligence Artificial Neural Network (ANN).

Acknowledgement

Thanks are due to Department of Engineering, Narula Institute of Technology for providing the $MATLAB$ facility.

References

1. "Calculation of AC Short circuit current at MMC-HVDC Converter Station" Xinjia Song, Qianhong Shi, Yipin Gong, Luhua Xing, Zhijun Wang, Lei Ding, 6th Asia Conference on Power and Electrical Engineering (ACPEE), 2021.
2. " Electrodynamics basics and duality principle" A. M. Ivanitckiy 2013 IX Internatioal Conference on Antenna Theory and Techniques.
3. "Research on Short Circuit Test of 500 kV Hybrid HVDC circuit breaker". Zhao Shu-Zhen; Zhang Jin-Xiang; Li Zhen-Dong; Yu Wen-Bo; Wang Yu-Qiang; Niu Xue-Fei; Kan Shi-Yang 2017 International Conference on Smart Grid and Electrical Automation (ICSGEA).
4. "Fast fourier transform in the spiral honeycomb image algebra". P. Sheridan;D.M. Alexander;K.S. Nunn-Clark. Third International Conference on Information Technology and Applications (ICITA'05). Vol – 1, 2005.
5. "MATLAB Programming Environment Based on Web". Liu Yu, 2018 IEEE 4th Information Technology and Mechatronics Engineering Conference (ITOEC).
6. "An efficient Fourier method for 3-D radon inversion in exact cone-beam CT reconstruction". S. Schaller;T. Flohr;P. Steffen, IEEE Transactions on Medical Imaging Year: 1998 Volume: 17, Issue: 2.
7. "DIFFT: A Fast and Accurate Algorithm for Fourier Transform Integrals of Discontinuous Functions" Yanhui Liu;Zaiping Nie;Qing Huo Liu, IEEE Microwave and Wireless Components Letters Year: 2008, Volume: 18, Issue: 11.

INDIAN JOURNAL OF THEORETICAL PHYSICS, VOL 71, NOS. 1 & 2, 2023

Reconstruct The Two Temperature Generalized Thermo-elasticity with Memory Dependent Derivative

Mohsin Islam

Department of Mathematics, Vidyasagar Metropolitan College, Kolkata-700006, West Bengal, India (mislam416@gmail.com)

Abstract: This present survey deals with a novel mathematical model of generalized thermoelasticity which investigates the transient phenomena in a piezoelastic half-space body in which the boundary is stress free and subjected to thermal loading in the context of two temperature generalized thermoelasticity theory (2TT). The three-phase-lag thermoelastic model (TPL), the Lord-Shulman model (LS) and the dual-phase lag (DPL) model are combined into a unified formulation. The memory-dependent derivative (MDD) is defined in an integral form of a common derivative on a slipping interval by incorporating the memory-dependent heat transfer. The basic equations have been written in the form of a vector-matrix differential equation in the Laplace-transform domain which is then solved by the state-space approach. The numerical inversion of the transform is carried out by a method based on Fourier-series expansion techniques. The numerical estimates of the quantities of physical interest are obtained and depicted graphically. The effect of the memory-dependent derivative on the solutions has been studied and the comparisons among different thermo elastic models are made.

Key Words: Memory dependent derivative, Generalized thermo piezo-elasticity, vector-matrix differential equation, Three-phase-lag thermo ealstic model, Dual-phase-lag model, Laplace transform.

1. Introduction

Diethelm[1] has developed the Caputo[2] derivative to be:

$$D_a^{\alpha} f(t) = \int_a^t K_{\alpha}(t-\xi) f^{(m)}(\xi) d\xi \qquad \dots (i)$$

with

$$K_{\alpha}(t-\xi) = \frac{(t-\xi)^{m-\alpha-1}}{\Gamma(m-\alpha)} \qquad \dots (ii)$$

where $f^{(m)}$ indicates the usual mth order derivative of the function. A memory-dependent derivative (MDD) has been introduced by Wang and Li[3]. The first order ($\alpha = 1$) derivative of function f is simply defined in an integral form involving a common derivative with a kernel function $K(t-\zeta)$ (chosen arbitrarily) on a slipping interval $[t-\tau, t]$ in the form

$$D_{\tau} f(t) = \frac{1}{\tau} \int_{t-\tau}^{t} K(t-\xi) f'(\xi) d\xi \qquad \dots (iii)$$

where $\tau\ (> 0)$ is the delay time. Generally, the memory effect needs weight $0 \leq K(t-\xi) \leq 1$ for $\xi \in [t-\tau, t]$ so that the magnitude of MDD $D_{\tau} f(t)$ is usually smaller than that of the common derivative $f'(t)$. As $\xi \in [t-\tau, t]$, we can understand easily that the function $f(\xi)$ takes values on the time interval $[t-\tau, t]$. Considering our present time as t, we can say that $[t-\tau, t]$ is our past. Thus we conclude the main feature of "memory-dependent derivative" that is the functional value in real time depends on the past time also. That is why D_{τ} is called a nonlocal operator whereas integer order derivative (or integration) is a local operator (i.e., it does not depend on past time). The kernel function $K(t-\xi)$ can be chosen freely, such as $1, [1-$

$(t-\xi)]$, $\left[1-\frac{t-\xi}{\tau}\right]^p$ for any real number p which may be more practical. They are a monotonically increasing function from 0 to 1 in the interval $[t-\tau, t]$. According to the nature of the problem, one can select a suitable kernel function of his/her choice. A special case: $K(t-\xi) \equiv 1$ and $\tau \longrightarrow 0$, we have

$$D_\tau f(t) = \frac{1}{\tau}\int_{t-\tau}^{t} f'(\xi)d\xi = \frac{f(t)-f(t-\tau)}{\tau} \to f'(t) \qquad \ldots (iv)$$

The above equation shows that $\frac{d}{dt}$ is a limiting case of D_τ as $\tau \to 0$. That is,

$$D_\tau f(t) \leq \left|\frac{\partial f}{\partial t}\right|.$$

Very recently, several problems in generalized thermo elasticity in the context of memory dependent derivatives have been reported in the studies[4–8]. Problems concerning three phase-lag thermo elastic model have been studied by many authors[9–11]. The present investigation is devoted to a study of thermo elastic stress, strain and conductive temperature in the piezo elastic half-space body under thermal shock in the context of memory dependent two-temperature generalized thermo elasticity theory. The governing equations of memory dependent two-temperature generalized thermo elasticity theory are obtained in the Laplace transform domain which are then solved by the state-space approach[12]. The inversion of the transformed solutions is carried out numerically by applying a method based on Fourier series expansion technique[13]. A complete and comprehensive analysis of the results have been presented for three-phase-lag (TPL), Lord-Shulman (LS) and dual-phase lag(DPL) models.

2. Formulation of the Problem

We now consider a thin semi-infinite piezoelectric body with stress free boundary occupying the space $x \geq 0$. At the near end of the body, a thermal effect is given which raises the temperature of this end to a prescribed temperature with known function, the direction of piezoelectric being parallel to x-axis.

We shall consider one-dimensional disturbance of the medium, so that the displacement vector $\vec{u}$ can be expressed in the following form

$$u_x = u(x,t), u_y = 0, u_z = 0. \tag{1}$$

Then the strain components in our case become

$$e = \frac{\partial u}{\partial x} \tag{2}$$

In the context of linear theory of Generalized thermo elasticity in absence of body forces and heat sources, the constitutive equation, the equation of motion, the Gauss's law and electric field relation and the heat equation in a unified form, can be written as

$$\sigma = c_{11}\frac{\partial u}{\partial x} - \beta\theta - hD, \tag{3}$$

$$c_{11}\frac{\partial^2 u}{\partial x^2} - \beta\frac{\partial \theta}{\partial x} = \rho\frac{\partial^2 u}{\partial t^2}, \tag{4}$$

Since there is no free charge inside the piezoelectric body from Gauss law, we have

$$\frac{\partial D}{\partial x} = 0. \text{ Hence } D = \text{constant}, \tag{5}$$

$$E = \frac{\partial \rho}{\partial x} \tag{6}$$

$$\left[K\left(1+\tau_T D_{\tau_T}+\frac{\tau_T^2 D_{\tau_T}^2}{2}\right)\frac{\partial}{\partial t}+K^*\left(1+\tau_v D_{\tau_v}\right)\right]\frac{\partial^2\phi}{\partial x^2}=$$

$$\left(1+t_1\tau_q D_{\tau_T}+\tau_2\frac{\tau_q^2}{2}D_{\tau_q}^2\right)\left(\rho c_E\ddot{\theta}+\beta\theta_0\frac{\partial\ddot{u}}{\partial x}\right). \quad (7)$$

The conductive temperature ϕ is given by

$$\phi\ -\ \theta\ =\ a\frac{\partial^2\phi}{\partial x^2} \quad (8)$$

where θ is the thermodynamic temperature, a, the temperature discrepancy, D the electric displacement component, θ_0 the reference temperature, ρ the density, c_E the specific heat, β the stress temperature coefficient, K^* an additional material constant, K the thermal conductivity, $\dot{v}\ =\ T, v$ the thermal displacement and $\tau_v^*=K+K_{\tau_v}^*$. Delay time τ_v is called the phase-lag of the thermal displacement gradient. Other delay time τ_T is called the phase-lag of the temperature gradient and τ_q is called the phase-lag of the heat flux. Here dot denotes derivative with respect to time. For $t_1=1,\ t_2$ = 1 the equation (7) reduces to TPL model, t_1 = 1, t_2 = 1, $K^*=0,\ \tau_T^2=0,\tau_T=0$ the equation reduces to LS model and for t_1 = 1, t_2 = 1, $K^*=0$ the equation reduces to DPL model.

We now introduce the following dimensionless variables

$$u'=c_0\eta u, x'\ =\ c_0\eta x,\qquad t'\ =\ c_0^2\eta t, \sigma'=\frac{\sigma}{c_{11}},$$

$$\theta'=\frac{\theta}{\theta_0}, \tau_T'=c_0^2\eta\tau_T,\ \tau_q'=c_0^2\eta\tau_q,\ \tau_v^{*'}=c_0^2\eta\tau_v^*,$$

$$\phi'=\frac{\phi}{\theta_0}, D'=\frac{h}{c_{11}}D,\qquad t_0'=c_0^2\eta t_0, K^{*\prime}=\frac{K^*}{\rho c_E c_0^2}$$

where

$$c_0^2 = \frac{c_{11}}{\rho} \text{ and } \eta = \frac{\rho c_E}{K}.$$

Substituting (2) into (3), (4) and using the dimensionless variables, equations (3), (4), (7) and (8) can be written in non dimensional form after omitting the primes as follows

$$\sigma = e - \alpha\theta - D, \tag{9}$$

$$\frac{\partial^2 e}{\partial x^2} - \alpha \frac{\partial^2 \theta}{\partial x^2} = \frac{\partial^2 e}{\partial t^2} \tag{10}$$

$$\left(1 + t_1 \tau_q D_{\tau_q} + t_2 \frac{\tau_q^2}{2} D_{\tau_1}^2\right)\left(\ddot{\theta} + \epsilon \ddot{e}\right) = \left[\left(1 + \tau_T D_{\tau_T} + \frac{\tau_T^2 D_{\tau_T}^2}{2}\right)\frac{\partial}{\partial t} + K^*\left(1 + \tau_v D_{\tau_v}\right)\right]\frac{\partial^2 \phi}{\partial x^2} \tag{11}$$

$$\theta = \phi - \omega \frac{\partial^2 \phi}{\partial x^2}, \tag{12}$$

where $\alpha = \frac{\beta \theta_0}{c_{11}}, \epsilon = \frac{\beta}{\rho c_E}, \omega = a c_0^2 \eta^2$.

The problem is to solve equations (9)-(12) subject to the boundary conditions (i) Stress free boundary

$$\sigma(0, t) = 0, \tag{13}$$

and (ii) Varying thermal load

$$\phi(0, t) = F(t). \tag{14}$$

where $F(t)$ is a known function of time t. The initial and regularity conditions can be written as

$$e = 0 = \theta = \phi \text{ at } t = 0, \tag{15}$$

$$\frac{\partial e}{\partial t} = \frac{\partial \theta}{\partial t} = \frac{\partial \phi}{\partial t} = 0 \text{ at } t = 0, \tag{16}$$

and

$$e(x,t) \to 0, \theta(x,t) \to 0, \phi(x,t) \to 0 \; as \; x \to \infty, t > 0. \tag{17}$$

From now on, the kernel function K(t − ξ) can be chosen freely as

$$K(t - \xi) = 1 - \frac{2b}{\tau}(t - \xi) + \frac{a^2}{\tau^2}(t - \xi)^2 = \begin{cases} 1, \text{if } a = b = 0 \\ 1 - \dfrac{t-\xi}{\tau} \text{ if } a = 0, b = \dfrac{1}{2} \\ \left(1 - \dfrac{t-\xi}{\tau}\right)^2 \text{ if } a = 1, b = 1 \end{cases} \tag{18}$$

where $\tau = \tau_T, \ \tau_q, \tau_v$, and a, b are constants.

From the view point of applications, different processes need different kernels to reflect their memory effects, so the kernel should be chosen freely.

3. Method of solution

Let

$$\bar{f}(x,s) = \int_0^\infty f(x,t)e^{-st}dt, \tag{19}$$

with $Re(p) > 0$ denotes the Laplace transform of $f(x,t)$.

Laplace transform on a memory-dependent derivative is :

$$\mathcal{L}\left[\tau D_\tau^i f(t)\right] = \mathcal{L}\left[\int_{t-\tau}^{t} K(t-\xi) f^i(\xi) d\xi\right] = s^{i-1}\mathcal{L}[f(t)]G(s,\tau) \tag{20}$$

where $i = 1, 2$ and $\tau = \tau_T, \ \tau_q, \tau_v$.

Here we get three functions $G(s,\tau_T), \ G(S,\tau_q), \ G(s,\tau_v)$.

$$G(s,\tau_T)(1-e^{s\tau_T})\left(1-\frac{2b}{\tau_T s}+\frac{2a^2}{\tau_T^2 s^2}\right)-\left(a^2-2b+\frac{2a^2}{\tau_T s}\right)e^{-s\tau_T} \quad (21)$$

$$G\left(s,\tau_q\right)(1-e^{s\tau_q})\left(1-\frac{2b}{\tau_q s}+\frac{2a^2}{\tau_q^2 s^2}\right)-\left(a^2-2b+\frac{2a^2}{\tau_q s}\right)e^{-s\tau_q} \quad (22)$$

$$G(s,\tau_v)(1-e^{s\tau_v})\left(1-\frac{2b}{\tau_v s}+\frac{2a^2}{\tau_v^2 s^2}\right)-\left(a^2-2b+\frac{2a^2}{\tau_v s}\right)e^{-s\tau_v} \quad (23)$$

Applying Laplace transform to the equations (9)-(14) we obtain,

$$\bar{\sigma}=\bar{e}-\alpha\bar{\theta}-\frac{D}{s}, \quad (24)$$

$$\frac{d^2\bar{e}}{dx^2}-\alpha\frac{d^2\bar{\theta}}{dx^2}=s^2\bar{e}, \quad (25)$$

$$\left[K^*\left(1+G(s,\tau_v)\right)+s\left(1+G(s,\tau_T)+s\frac{\tau_T}{2}G(s,\tau_T)\right)\right]\frac{d^2\bar{\phi}}{dx^2}$$
$$=s^2\left(1+t_1G(s,\tau_1)+t_2s\frac{\tau_q}{2}G\left(s,\tau_q\right)\right)(\bar{\theta}+\epsilon\bar{e}) \quad (26)$$

$$\bar{\theta}=\bar{\phi}-\omega\frac{d^2\bar{\phi}}{dx^2} \quad (27)$$

$$\bar{\phi}(0,s)=\bar{F}(s) \quad (28)$$

and

$$\bar{\sigma}(0,s)=\bar{\sigma}_0(s)=0 \quad (29)$$

Eliminating $\bar{\theta}$ between (26) and (27) we get

$$\frac{d^2\bar{\phi}}{dx^2}=l\bar{\phi}+l\epsilon\bar{e} \quad (30)$$

where $l=\frac{a_3}{1+a_2\omega}$ and

$$a_3 = \frac{s^2(1 + t_1 G(2, \tau_q) + t_2 s \frac{\tau_q}{2} G(s, \tau_q)}{[K^* \left(1 + G(s, \tau_v) + s \left(1 + g(s, \tau_T) + s \frac{\tau_T}{2} G(s, \tau_T)\right)\right]}$$

Again using (Eq. 30) in Eq. (27) we get

$$\bar{\theta} = (1 - l\omega)\bar{\phi} - l\omega \in \bar{e} \tag{31}$$

Now from Eq. (25) we get

$$\frac{d^2\bar{e}}{dx^2} = M\bar{\phi} + N\bar{e} \tag{32}$$

$$\text{where } M = \frac{\alpha(1 - l\omega)l}{1 + l \in \alpha\omega}, \quad N = \frac{s^2 + \alpha(1 - l\omega)l \in}{1 + l \in \alpha\omega}.$$

4. State-Space Approach

Equations (30) and (32) can be written in vector-matrix differential equation as

$$\frac{d^2\bar{V}(x, s)}{dx^2} = A(s)\bar{V}(x, s) \tag{33}$$

where $\bar{V}(x, s) = \begin{pmatrix} \bar{\phi} \\ \bar{e} \end{pmatrix}$ and $A(s) = \begin{pmatrix} l & l\epsilon \\ M & N \end{pmatrix}$.

Hence the solution of equation (33) is

$$\bar{V}(x, s) = \bar{V}(0, s)e^{-\sqrt{A(s)x}} \tag{34}$$

where $\bar{V}(0, s) = \begin{pmatrix} \bar{\phi}_0 \\ \bar{e}_0 \end{pmatrix}$ and

$$\bar{\phi}_0 = \bar{F}(s) \tag{35}$$

$\bar{e}_0 = \bar{e}(0, s)$.

The characteristic equation corresponding to matrix A is

$$\lambda^2 - (l + N)\lambda + (lN - \in lM) = 0. \tag{36}$$

The roots λ_1, λ_2 are given by

$$\lambda_1 + \lambda_2 = l + N, \tag{37}$$

$$\lambda_1\lambda_2 = lN - \epsilon lM$$

Now spectral decomposition of $A(s)$ is

$$A(s) = \lambda_1 E_1 + \lambda_2 E_2 \tag{38}$$

where E_1 and E_2 are called the projectors of $A(s)$ and they satisfy the following conditions

$E_1 + E_2 = I; I$ being the identity matrix,

$E_1 + E_2 =$ zero matrix,

$E_i^2 = E_i,$ for $i = 1, 2.$

Then we have

$$\sqrt{A(s)} = \sqrt{\lambda_1}E_1 + \sqrt{\lambda_2}E_2 \tag{39}$$

where

$$E_1 = \frac{1}{\lambda_1 - \lambda_2}\begin{pmatrix} l - \lambda_2 & \in l \\ \dfrac{(\lambda_1 - l)(\lambda_2 - l)}{l \in} & \lambda_1 - l \end{pmatrix}$$

And

$$E_2 = \frac{1}{\lambda_1 - \lambda_2}\begin{pmatrix} \lambda_1 - l & -\epsilon l \\ \dfrac{(\lambda_1 - l)(\lambda_2 - l)}{l\epsilon} & l - \lambda_2 \end{pmatrix}$$

Therefore, we get

$$B(s) = \sqrt{A(s)} = \frac{1}{\sqrt{\lambda_1} + \sqrt{\lambda_2}}\begin{pmatrix} l + \sqrt{\lambda_1\lambda_2} & l \in \\ M & N + \sqrt{\lambda_1\lambda_2} \end{pmatrix} \tag{40}$$

Now the solution of (33) can be written as

$$\bar{V}(x,s) = \bar{V}(0,s)e^{[-B(s)x]} \tag{41}$$

To find the form of the matrix $\exp[-B(s)x]$ we now apply Cayley-Hamilton theorem. The characteristic equation of the matrix $B(s)$ can be written as follows.

$$P^2 - P\left(\sqrt{\lambda_1} + \sqrt{\lambda_2}\right) + \sqrt{\lambda_1}\sqrt{\lambda_2} = 0 \tag{42}$$

The roots of this equation, taken as P_1, P_2 are as follows

$$P_1 = \sqrt{\lambda_1} \text{ and } P_2 = \sqrt{\lambda_2} \tag{43}$$

The Taylor series expansion for the matrix exponential $\exp[-B(s)x]$ is given by Bahar and Hetnarski[13.]

$$\exp[-B(s)x] = \sum_{n=0}^{\infty} \frac{[-B(s)x]^n}{n} \tag{44}$$

We can express B^2 and higher powers of the matrix B in terms of I and B where I is unit matrix of second order[13]. Then the infinite series in Eq. (44) can be reduced to the following form

$$exp[-B(s)x] \;=\; b_0(x,s)I \;+ b_1(x,s)B(s), \tag{45}$$

where b_0, b_1 are coefficients depending on s and x.

The characteristic roots P_1, P_2 of the matrix B must satisfy equation (45). Then we have

$$exp[-P_1x] \;=\; b_0 \;+\; b_1P_1, \tag{46}$$

$$exp[-P_2x] \;=\; b_0 \;+\; b_1P_2. \tag{47}$$

Solving equations (46) and (47) we get b_0, b_1 as follows

$$b_0 = \frac{P_1e^{-P_2x} - P_2e^{-P_1x}}{P_1 - P_2} \tag{48}$$

$$b_1 = \frac{e^{-P_1 x} - e^{-P_2 x}}{P_1 - P_2} \tag{49}$$

Hence, equation (45) can be written as,

$$exp[-B(s)x] = H(x,s) = [h_{ij}(x,s)], i,j = 1,2, \tag{50}$$

where

$$h_{11} = \frac{(P_1^2 - l)e^{-P_2 x} - (P_2^2 - l)e^{-P_1 x}}{P_1^2 - P_2^2} \tag{51}$$

$$h_{12} = \frac{\varepsilon l(e^{-P_1 x} - e^{-P_2 x})}{P_1^2 - P_2^2} \tag{52}$$

$$h_{21} = \frac{M(e^{-P_1 x} - e^{-P_2 x})}{P_1^2 - P_2^2} \tag{53}$$

$$h_{22} = \frac{(P_1^2 - N)e^{-P_1 x} - (P_2^2 - N)e^{-P_2 x}}{P_1^2 - P_2^2} \tag{54}$$

Using equation (50) in equation (41) we get

$$\bar{V}(x,s) = \left[h_{ij}(x.s)\right]\bar{V}(o,s),$$

which can be written as

$$\begin{pmatrix} \bar{\phi} \\ \bar{e} \end{pmatrix} = \begin{pmatrix} h_{11} & h_{12} \\ h_{21} & h_{22} \end{pmatrix} \begin{pmatrix} \bar{\phi}_0 \\ \bar{e}_0 \end{pmatrix} \tag{55}$$

Therefore the solutions for $\bar{\phi}$ and $\bar{e}$ are obtained from equation (55) as follows

$$\bar{\phi} = \phi_1 e^{-P_2 x} - \phi_2 e^{-P_1 x} \tag{56}$$

$$\bar{e} = e_1 e^{-P_2 x} - e_2 e^{-P_1 x} \tag{57}$$

where

$$\phi_1 = \frac{[(P_1^2 - l)\bar{\phi}_0 - \epsilon l \bar{e}_0]}{P_1^2 - P_2^2}, \qquad \phi_2 = \frac{[(P_2^2 - l)\bar{\phi}_0 - \epsilon l \bar{e}_0]}{P_1^2 - P_2^2}$$

$$e_1 = \frac{[(P_1^2 - N)\bar{e}_0 - M\bar{e}_0]}{P_1^2 - P_2^2}, \qquad e_2 = \frac{[(P_2^2 - N)\bar{e}_0 - M\bar{e}_0]}{P_1^2 - P_2^2}$$

Using equations (56) and (57) into equation (31) we get

$$\bar{\theta} = \phi_1 e^{-P_2 x} - \phi_2 e^{-P_1 x} \tag{58}$$

where

$$\theta_1 = (1 - \omega l)\phi_1 - \omega l e_1, \qquad \phi_2 = (1 - \omega l)\phi_2 - \omega l e_2$$

Now the solution for stress $\bar{\sigma}$ is obtained from equation (24) by using equations (57) and (58) as follows

$$\bar{\sigma} = \sigma_1 e^{-P_2 x} - \sigma_2 e^{-P_1 x} - \frac{D}{s}, \tag{59}$$

where

$$\sigma_1 = e_1 - \alpha\theta_1, \qquad \sigma_2 = (1 - \omega l)\phi_2 - \omega l e_2.$$

which completes the solution in the Laplace transform domain.

4.1 Thermal shock

We take the thermal load in the following form

$$F(t) = F_0 H(t)$$

where F_0 is constant and $H(t)$ the Heaviside unit step function. Taking Laplace transform

we have

$$\bar{\phi}_0 = F = \frac{F_0}{s} \tag{60}$$

and

$$\bar{e}_0 = \frac{1}{1 + l\omega\epsilon\alpha}\left[\frac{\alpha(1 - l\omega)F_0}{s} + \frac{D}{s}\right] \tag{61}$$

Thus we get the complete solution of the thermal shock problem on the Laplace transform domain using equations (60) and (61) into the equations (56) to (59).

5. Numerical Results and Discussion

To get the solutions for stress component (σ), strain component (e) and conductive temperature (ϕ) in the space-time domain we have to apply the Laplace inversion formula to the Eqs. (56), (57) and (58) respectively, which have been done numerically using a method based on Fourier series expansion technique.

For computational purposes the values of material constants have been taken as follows[1]

$$F_0 = 1, \epsilon = 0.003887, \alpha = 0.036991, \omega = 0.1, K^* = 7.$$

Here in this paper we have considered three-phase-lag model. Now for this model the solution of the heat conduction law is stable if

$$\frac{2K\tau_T}{\tau_q} > \tau_v^* > K^*\tau_q \tag{62}$$

where $\tau_v^* = K^*\tau_v + K$. We have assumed the values of these phase lag parameters in our paper in the way that they have satisfied the above condition. And hence for numerical calculation we have taken $\tau_q = 0.01, \tau_T = 0.2, \tau_v = 1.01$.

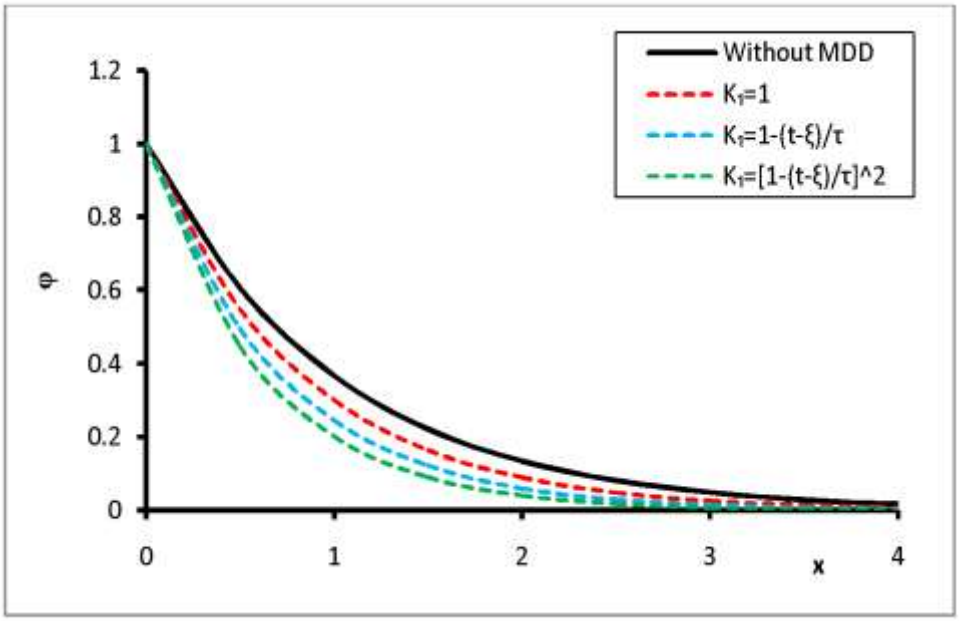

Figure 1(a)
Effect of different kernel of MDD (colored lines) on conductive temperature distribution for $\tau = 0.001$*, two-temperature TPL model.*

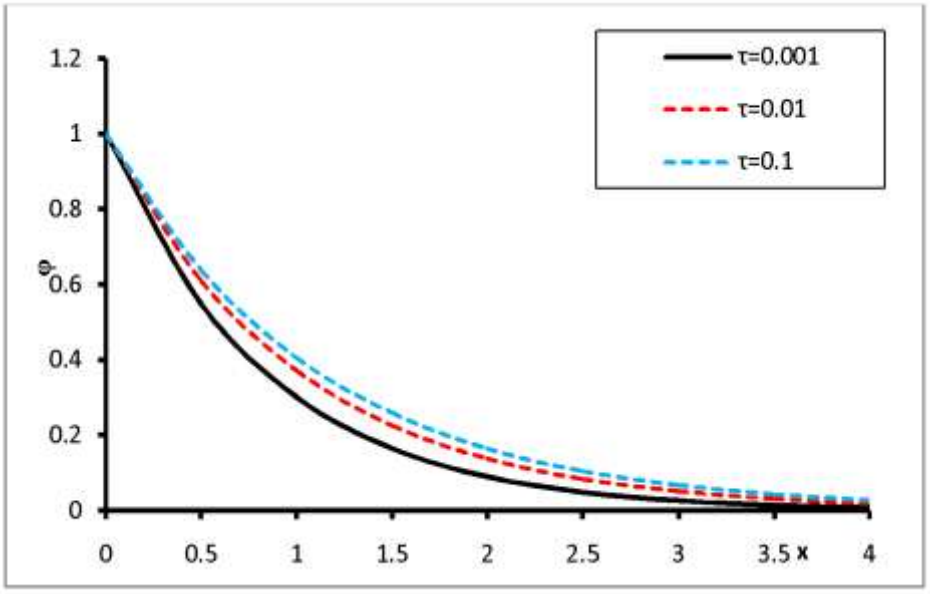

Figure 1(b)
Effect of delay times on conductive temperature distribution for two-temperature TPL model.

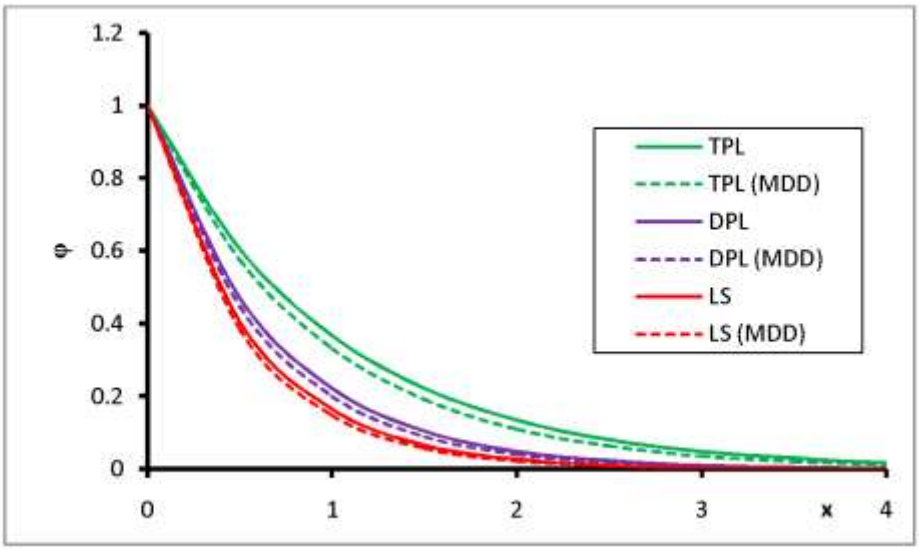

Figure 1(c)
Comparison of three models for conductive temperature distribution in presence and absence of MDD for two-temperature theory.

Figures 1.(a)-(c) represent the variations of conductive temperature ϕ against x for $t = 0.25, D = 0.15, \omega = 0.1$ for different kernel functions using the three-phase lag model (TPL), for different delay time τ using the three-phase lag model (TPL) and using different models (TPL, LS and DPL) respectively. As seen from these figures that ϕ is maximum at $x = 0.0$, which satisfy the theoretical boundary condition. Also, its magnitude, in each case, gradually decreases with the increase of x, which is physically plausible. The magnitude of the profile of the conductive temperature is larger for $K(t - \xi) = 1$ than that of $K(t - \xi) = 1 - \frac{t-\xi}{\tau}$, magnitude of which is larger compared to $K(t - \xi) = \left(1 - \frac{t-\xi}{\tau}\right)^2$

Figure 1.(b) is plotted to show the variation of the conductive temperature ϕ against x for different delay time τ ($\tau = 0.001, 0.01$ and

0.1) keeping fixed the kernel function as $K = 1$ and using the three-phase lag model (TPL). It is seen that rise in magnitude of the delay time τ also increases the magnitude of the temperature distribution.

Figure 1.(c) is plotted to show the variation of the conductive temperature ϕ for TPL, LS and DPL models. It is clear from the figure that the numerical results for the temperature distribution (for three models) are found to satisfy the theoretical boundary condition. The magnitude of conductive temperature ϕ for TPL model is greater than that of DPL model which is again greater than that of LS model for all x.

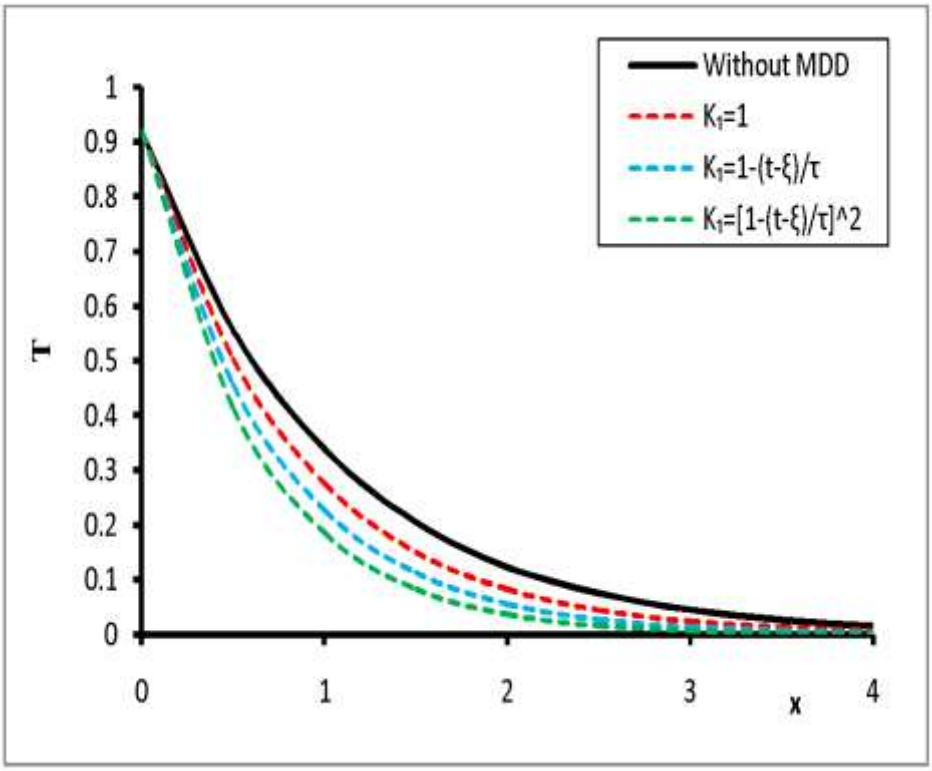

Figure 2(a)
Effect of different kernel of MDD (colored lines) on thermodynamic temperature distribution for $\tau = 0.002$, two-temperature TPL model.

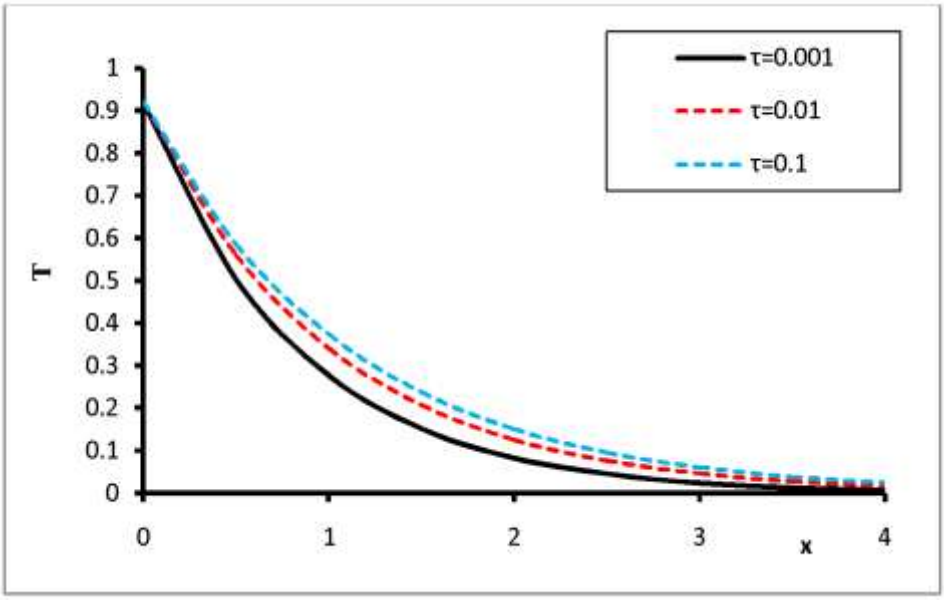

Figure 2(b)
Effect of delay times on thermodynamic temperature distribution for two-temperature TPL model.

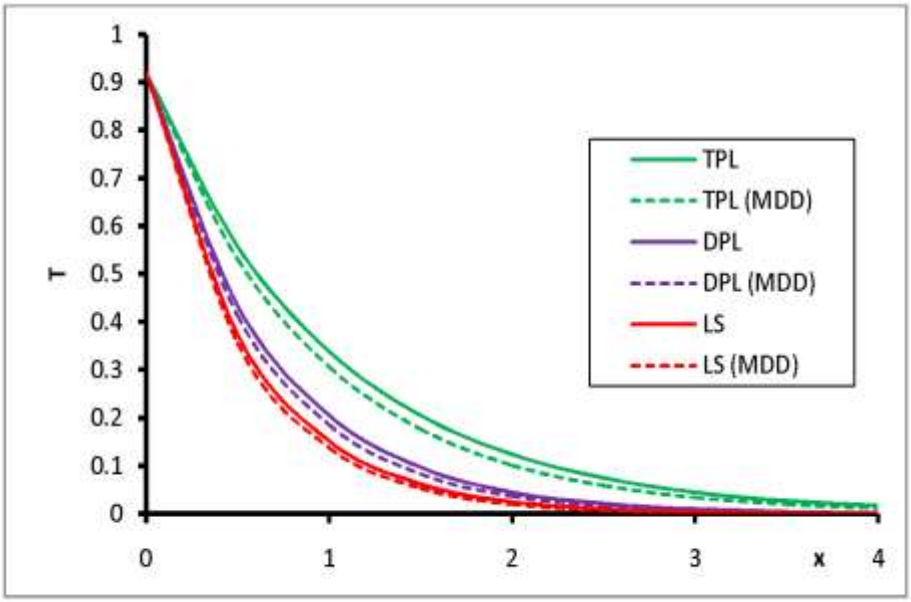

Figure 2(c)
Comparison of three models for thermodynamic temperature distribution in presence and absence of MDD for two-temperature theory.

Figures 2.(a)-(c) represent the variations of thermodynamic temperature θ against x for $t = 0.25, D = 0.15, \omega = 0.1$ for different kernel functions using the three-phase lag model (TPL), for different delay time τ using the three-phase lag model (TPL) and using different models (TPL, LS and DPL) respectively. As seen from these figures that θ is maximum at $x = 0.0$ and gradually decreases with the increase of x. The fact is expected as we applied the thermal shock at the boundary ($x = 0$). Also for finite speed of heat propagation phenomenon has been supported by the finite value of temperature (both conductive and thermodynamic) at some distance from $x = 0$. In this context, it is to be noted that for one temperature case ($\omega = 0$) thermodynamic temperature and conductive temperature be the same.

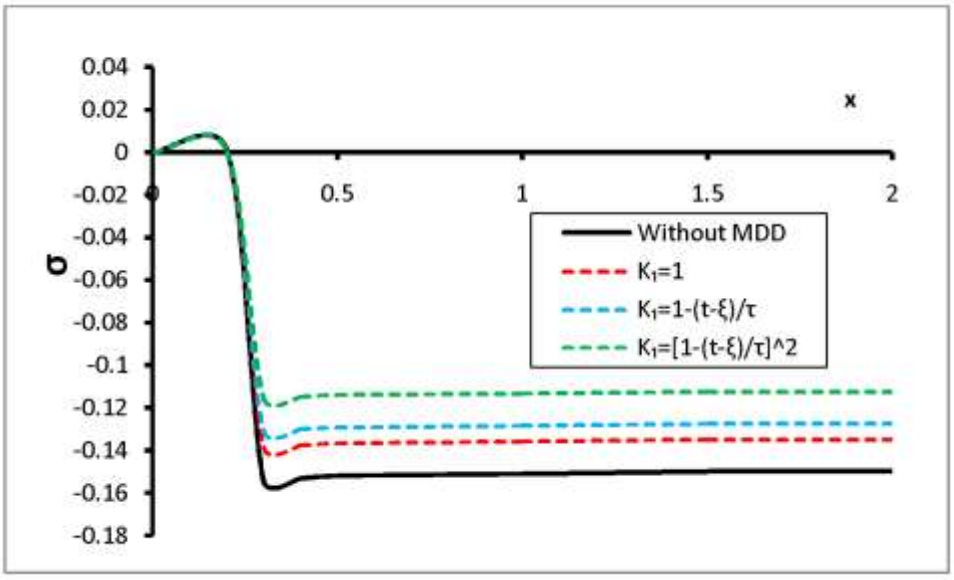

Figure 3(a)
Effect of different kernel of MDD (colored lines) on stress distribution for $\tau = 0.003$, *two-temperature TPL model.*

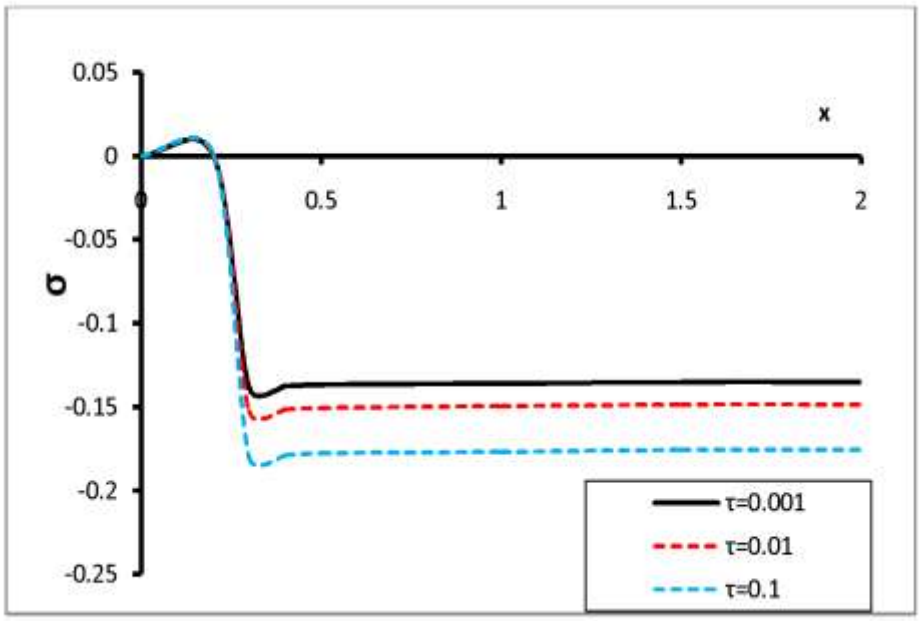

Figure 3(b)
Effect of delay times on stress distribution for two-temperature TPL model.

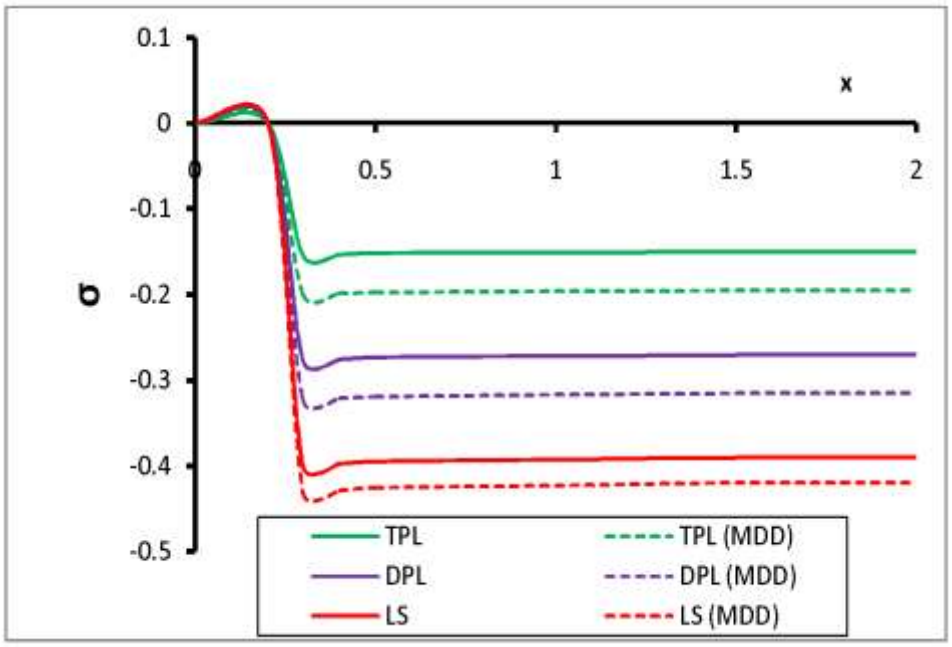

Figure 3(c)
Comparison of three models for stress distribution in presence and absence of MDD for two-temperature theory.

In Figure 3.(a) the stress σ is plotted against x for $\tau = 0.001$ and for various kernel functions, as mentioned earlier. The qualitative behavior of stress distribution is almost the same for all the kernel functions but the magnitude of the σ is larger for $K(t - \xi) = 1$. The steep jump of σ occurs at a particular value of x. Figure 3.(b) depict the graph of the stress σ verses the space variable x for different delay time $\tau, K = 1$ and using the TPL model. Significant difference in the stress is noticed for different values of the non-dimensional delay time parameter. Numerical results shows that the magnitude of stress σ is greater for $\tau = 0.1$ and it has been found that magnitude of the stress distribution increases as the delay time τ increases. Figure 3.(c) represents the graph of the stress distribution σ against x for the three models (TPL, DPL and LS models).

References

1. Diethelm K (2010) The Analysis of Fractional Differential Equations: An Applicationoriented Exposition Using Differential Operators of Caputo Type, Springer, Berlin.
2. Caputo M (1967) Linear models of dissipation whose Q is almost frequency independent II. Geophys. J. Int. 13(5): **529-539.**
3. Wang J.-L., Li H-F (2011) Surpassing the fractional derivative: Concept of the memorydependent derivative. Comput. Math. Appl. 62(3): **1562-1567**.
4. Yu Ya-Jun, Wei H., Xiao-Geng T (2014) ”A novel generalized thermoelasticity model based on memory-dependent derivative.” International Journal of Engineering Science 81: **123-134.**
5. Islam M, Mondal S (2020) Memory response in a two-dimensional transversely isotropic thick plate with varying heat source. Z Angew Math Mech 101(6).

6. Mondal S, Sur A, Kanoria M (2019) Transient response in a piezoelastic medium due to the influence of magnetic field with memory-dependent derivative. Acta Mechanica 230(7): **2325-2338**.

7. Mondal S, Sur A, Kanoria M (2019) A memory response in the vibration of a microscale beam induced by laser pulse. J. Therm. Stresses 42(11): **1415-1431.**

8. Mondal S, Sur A, Kanoria M (2019) Transient heating within skin tissue due to timedependent thermal therapy in the context of memory dependent heat transport law. Mech. Based Des. Struct. Mach 1-15 doi: **10**.1080/15397734.2019.1686992.

9. Islam M, Kanoria M (2011) Study of dynamical response in a transversely isotropic thick plate due to heat source. J. Thermal Stresses 34: **702-723**.

10. Islam M, Kar A, Kanoria M (2013) Two-Temperature Generalized Thermoelasticity in a Fiber-Reinforced Hollow Cylinder Under Thermal Shock. International Journal for Computational Methods in Engineering Science and Mechanics **14**: 367-390.

11. Islam M, Kar A, Kanoria M (2014) Thermoelastic response in a symmetric spherical shell. Acta Mechanica **225**: 2841-2864.

12. Bahar LY, Hetnarski RB(1978) State space approach to thermoelasticity. J. Thermal Stresses. **1**: 135-145.

13. Honig G, Hirdes U(1984) A method for the numerical inversion of Laplace transform. J. Comp. Appl. Math. **10**: 113-132.

14. Islam M, Kanoria M (2014) One-dimensional problem of a fractional order twotemperature generalized thermo-piezoelasticity. Mathematics and Mechanics of Solids 19(6): **672-693**.

———

One Day Seminar on 'Recent Trends of Physics & Mathematics was held on 7th July, 2023 to celebrate 71st Anniversary of CITP in collaboration with Dept. of Mathematics, Vidyasagar Metropolitan College, Kolkata. The following Memorial Lectures were presented in the Seminar.

1. Prof. P.P. Chattarji Memorial Lecture on 'Different aspects of Social Network Analysis and their Application.

   Speaker : Prof. Kajal De, Hon'ble Vice-Chancellor, Diamond Harbour Womens University, West Bengal

2. Prof. K. C. Kar Memorial Lecture on 'Quantum Materials – a new playground for exiting Physics.

   Speaker : Prof. Pritam Deb, Dept. of Physics, Tezpur University, Assam.

About 60 UG students and teachers from different Colleges of Kolkata participated in the Seminar. Both the lectures were highly interactive. Participants asked interesting questions to understand the subjects. The speaker encouraged the advanced learners. The seminar ended with vote of thanks by Dr. Mohasin Islam, Head of the dept. of Mathematics, Vidyasagar Metropolitan College, Kolkata.

———

INFORMATION TO AUTHORS

Manuscripts should represent results of original works on theoretical physics or experimental physics with theoretical background or on applied mathematics. Letters to the Editor and Review articles in emerging areas are also published. Submission of the manuscript will be deemed to imply that it has not been published previously and is not under consideration for publication elsewhere (either partly or wholly) and further that, if accepted, it will not be published elsewhere. It is the right of the Editorial Board to accept or to reject the paper after taking into consideration the opinions of the references.

Manuscripts may be submitted in pdf/MS word format to **admin@citphy.org or susil_vcsarkar@yahoo.co.in** Online submission of the paper through our **website: www.citphy.org** is also accepted. The file should be prepared with 2.5 cm margin on all sides and a line spacing of 1.5.

The title of the paper should be short and self-explanatory. All the papers must have an abstract of not more than 200 words, the abstract page must not be a part of the main file. Abstract should be self-contained. It should be clear, concise and informative giving the scope of the research and significant results reported in the paper. Below the abstract four to six key words must be provided for indexing and information retrieval.

The main file should be divided into sections (and sub-sections, if necessary) starting preferably with introduction and ending with conclusion. Displayed formula must be clearly typed (with symbols defined) each on a separate line and well-separated from the adjacent text. Equations should be numbered with on the right-hand side consecutively throughout the text. Figures and Tables with captions should be numbered in Arabic numerals in the order of occurrence in the text and these should be embedded at appropriate places in the text. Associated symbols must invariably follow SI practice.

References should be cited in the text by the Arabic numerals as superscript. All the references to the published papers should be numbered serially by Arabic numerals and given at the end of the paper. Each reference should include the author's name, title, abbreviated name of the journal, volume number, year of publication, page numbers as in the simple citation given below :

For Periodicals : Sen, N. R. - On decay of energy spectrum of Isotopic Turbulence, 1. Appl. Phys. **28,** No. 10, 109-110 (1999).

1. Mikhilin, S. G. - Integral Equations, Pergamon Press, New York (1964).
2. Hinze, A. K. - Turbulence Study of Distributed Turbulent Boundary Layer Flow, Ph. D, Thesis, Rorke University (1970).

The corresponding author will receive page proof, typically as a pdf file. The proof should be checked carefully and returned to the editorial office within two or three days. Corrections to the proof should be restricted to printing errors and made according to standard practice. At this stage any modifications (if any) made in the text should be highlighted.

To support the cost of publication of the journal, the authors (or their Institutions) are requested to pay publication charge ₹ 200/- per printed page for authors of Indian Institutes and US$ 20 for others. Publication charges to be sent directly to **CALCUTTA INSTITUTE OF THEORETICAL PHYSICS, 'BIGNAN KUTIR', 4/1 MOHAN BAGAN LANE, KOLKATA-700004, INDIA.**

A pdf of the final publisher's version of the paper will be sent to the corresponding author.

All communications are to be sent to the Secretary, Calcutta Institute of Theoretical Physics, 'BignanKutir', 4/1, Mohan Bagan Lane, Kolkata-700004, India. E-mail:susil_vcsarkar@yahoo.co.in

For details please visit our website www.citphy.org

INDIAN JOURNAL OF THEORETICAL PHYSICS

BOARD OF EDITORS

CALCUTTA INSTITUTE OF THEORETICAL PHYSICS

(Formerly, Institute of Theoretical Physics)

[Established in 1953 by Late Prof. K. C. Kar, D. Sc.]

PUBLICATIONS
OF
CALCUTTA INSTITUTE OF THEORETICAL PHYSICS
"BIGNAN KUTIR"
4/1, Mohan Bagan Lane, Kolkata-700 004, India
Phone : +91-33-25555726

INDIAN JOURNAL OF THEORETICAL PHYSICS (ISSN : 0019-5693)
Research Journal containing Original Papers, Review Articles and Letters to the Editor is published quarterly in March, June, September and December and circulated all over the world.

Subscription Rates
₹ 1500 per volume (for Bonafide Indian Party)
US$ 350 (for Foreign Party)

Back Volume Rates
₹ 1500 per volume (for Bonafide Indian Party)
US$ 350 per volume or Equivalent Pounds per volume

Books Written by Prof. K. C. Kar, D. Sc.

- **INTRODUCTION TO THEORETICAL PHYSICS [Vol. I and Vol. II (Acoustics)]** Useful to students of higher physics
  Price :₹ 60 or US $ 10 per volume
- **WAVE STATISTICS : Its principles and Applications [Vol. I and Vol. II]** Useful to Post Graduate and Research students
  Price :₹ 80 or US $ 12
- **STATISTICAL MECHANICS : PRINCIPLES AND APPLICATIONS [Vol. I and Vol. II]** Useful to Advanced students of theoretical Physics
  Price :₹ 120 or US $ 15
- **A NEW APPROACH TO THE THEORY OF RELATIVITY [Vol. I and Vol. II]** Useful to Post Graduate and advanced students
  Price :₹ 50 or US $ 8

Order may be sent directly to Calcutta Institute of Theoretical Physics
"BignanKutir", 4/1, Mohan Bagan Lane, Kolkata-700 004, India